Lower Colorado River Multi-Species Conservation Program

Balancing Resource Use and Conservation

Genetic Characterization of the California Leaf-nosed Bat (*Macrotus californicus*) Along the Lower Colorado River

Final Report

February 2019

Work conducted under LCR MSCP Work Task C43

Lower Colorado River Multi-Species Conservation Program Steering Committee Members

Federal Participant Group

Bureau of Reclamation
U.S. Fish and Wildlife Service
National Park Service
Bureau of Land Management
Bureau of Indian Affairs
Western Area Power Administration

Arizona Participant Group

Arizona Department of Water Resources
Arizona Electric Power Cooperative, Inc.
Arizona Game and Fish Department
Arizona Power Authority
Central Arizona Water Conservation District
Cibola Valley Irrigation and Drainage District
City of Bullhead City
City of Lake Havasu City
City of Mesa
City of Somerton
City of Yuma
Electrical District No. 3, Pinal County, Arizona
Golden Shores Water Conservation District
Mohave County Water Authority
Mohave Valley Irrigation and Drainage District
Mohave Water Conservation District
North Gila Valley Irrigation and Drainage District
Town of Fredonia
Town of Thatcher
Town of Wickenburg
Salt River Project Agricultural Improvement and Power District
Unit "B" Irrigation and Drainage District
Wellton-Mohawk Irrigation and Drainage District
Yuma County Water Users' Association
Yuma Irrigation District
Yuma Mesa Irrigation and Drainage District

Other Interested Parties Participant Group

QuadState Local Governments Authority
Desert Wildlife Unlimited

California Participant Group

California Department of Fish and Wildlife
City of Needles
Coachella Valley Water District
Colorado River Board of California
Bard Water District
Imperial Irrigation District
Los Angeles Department of Water and Power
Palo Verde Irrigation District
San Diego County Water Authority
Southern California Edison Company
Southern California Public Power Authority
The Metropolitan Water District of Southern California

Nevada Participant Group

Colorado River Commission of Nevada
Nevada Department of Wildlife
Southern Nevada Water Authority
Colorado River Commission Power Users
Basic Water Company

Native American Participant Group

Hualapai Tribe
Colorado River Indian Tribes
Chemehuevi Indian Tribe

Conservation Participant Group

Ducks Unlimited
Lower Colorado River RC&D Area, Inc.
The Nature Conservancy

Lower Colorado River Multi-Species Conservation Program

Genetic Characterization of the California Leaf-nosed Bat (*Macrotus californicus*) Along the Lower Colorado River

Final Report

Prepared by:

Jeff Hill, Wildlife Group

Lower Colorado River
Multi-Species Conservation Program
Bureau of Reclamation
Lower Colorado Region
Boulder City, Nevada
http://www.lcrmscp.gov

February 2019

Hill, J. 2019. Genetic Characterization of the California Leaf-nosed Bat (*Macrotus californicus*) Along the Lower Colorado River, Final Report. Lower Colorado River Multi-Species Conservation Program, Bureau of Reclamation, Boulder City, Nevada.

ACRONYMS AND ABBREVIATIONS

AMOVA	analysis of molecular variance
BIC	Bayesian information criterion
DAPC	Discriminant Analysis of Principal Components
DNA	deoxyribonucleic acid
F_{ct}	among-group fixation index
F_{sc}	among-population within-group fixation index
F_{st}	among-population fixation index
gDNA	double-stranded genomic DNA
IUCN	International Union for the Conservation of Nature
LCR	lower Colorado River
LCR MSCP	Lower Colorado River Multi-Species Conservation Program
mm	millimeter(s)
mtDNA	mitochondrial deoxyribonucleic acid
N_e	effective population size
NGS	Next-generation sequencing
PC	principal component
PCR	polymerase chain reaction

Symbols

°C	degrees Celsius
>	greater than
<	less than
µL	microliter(s)
	number
π	pi
(θ)	theta

CONTENTS

Page

Abstract iii

Introduction 1
Life History 3
Distribution 3
Physical Description and Taxonomic History 3
Habitat, Foraging, and Reproduction 5
Conservation Status 5
Methods 6
Sample Collection and Sequencing 6
Genetic Analyses 8
Results 9
Sequencing 9
Genetic Analyses 12
Discussion 27
Literature Cited 29

Tables

Table Page

1 Mitochondrial haplotype list 11
2 Whole genome sequencing results for six individuals 12
3 Microsatellites and associated primer information 12
4 Summary of chi-square test of Hardy-Weinberg equilibrium 13
5 Mitochondrial pooled sequence statistics 14
6 Sequence statistics for northern range samples 14
7 Sequence statistics for southern range samples 14
8 Mitochondrial AMOVA results 15
9 Microsatellite AMOVA results 16
10 Tajima's neutrality test for all sample 17
11 Tajima's neutrality test for northern range samples 17
12 Tajima's neutrality test for southern range samples 17

Figures

Figure Page

1 International Union for the Conservation of Nature distribution map (Solari 2018) for the California leaf-nosed bat. 4
2 Sample localities of the California leaf-nosed bat. 7
3 Mitochondrial haplotype map. 10
4 Mitochondrial median joining network. 15
5 Matrix of pairwise F_{st} values for mitochondrial data. 18
6 Matrix of pairwise differences within and between populations, and Nei's distance for mitochondrial data. 19
7 Mismatch distribution for all mitochondrial samples (n = 99). 20
8 Mismatch distribution for mitochondrial data from the United States (n = 76). 21
9 Mismatch distribution for mitochondrial data from the Baja California Sur, Mexico, and Sonora, Mexico (n = 23). 22
10 Mean natural logarithm probability of microsatellite data for K = 1 to K = 20 across 20 runs. 23
11 STRUCTURE results for K = 2 clusters. 23
12 Matrix of pairwise F_{st} values for microsatellite data. 24
13 Matrix of pairwise differences and Nei's distance for microsatellite data. 25
14 Scatterplot showing individuals colored by clusters with inertia ellipses (based on four PCs). 26
15 STRUCTURE type DAPC plot: Individual bars labeled by sample site (four PCs). 26

Attachments

Attachment

1 Supplemental Tables

ABSTRACT

This project aims to describe the current genetic diversity and demographic history of the California leaf-nosed bat (*Macrotus californicus)* along the lower Colorado River (LCR) and how populations along the river relate to the genetic diversity across the species' range. By contributing knowledge of the poorly understood demographics of the California leaf-nosed bat, we hope to assist with future conservation considerations for the species. A total of 916 base pairs of the cytochrome *b* mitochondrial deoxyribonucleic acid (mtDNA) gene were sequenced for 102 individuals from 17 localities along the LCR, the Southwestern United States, Baja California Sur, Mexico, and northern mainland Mexico. There were 18 haplotypes identified across the range, with 5 haplotypes present in the samples taken from the LCR, and 3 haplotypes unique to the river. Sequence statistics for microsatellite data revealed higher genetic variation in samples from the southern portion of the range. Genotypic clustering analysis of 5 microsatellite loci across 88 individuals from 19 localities allowed us to infer two genetic groups present in the species' range, with none being unique to the LCR and surrounding areas. Mismatch distributions and Tajima's neutrality test indicated low levels of genetic variation in the northern range of the species. Analysis of molecular variance runs indicated higher levels of structuring in mtDNA versus genomic microsatellite DNA. Both program STRUCTURE and Discriminant Analysis of Principal Components analyses showed little evidence of geographic structuring for nuclear markers.

INTRODUCTION

The California leaf-nosed bat (*Macrotus californicus*) is one of two bat species under evaluation by the Lower Colorado River Multi-Species Conservation Program (LCR MSCP). The LCR MSCP is a 50-year interagency partnership comprised of Federal and non-Federal stakeholders, and implemented by the Bureau of Reclamation to conserve habitat while accommodating present water diversions and power production occurring along the lower Colorado River (LCR). The program provides authorization for incidental take of 27 covered and 5 evaluation species under Section 10(a)1(B) of the Endangered Species Act. Under the LCR MSCP, evaluation species are those that could become listed as threatened or endangered under the Endangered Species Act in the future and for whom insufficient information exists to determine the effects of covered activities or to develop conservation measures. This project is being conducted as part of the research to determine the status of evaluation species within the LCR MSCP planning area.

The California leaf-nosed bat is a non-migratory, colonial, cave-roosting bat (Bradshaw 1961). This species is not readily detected using acoustic surveys because of its low decibel calls and the similarity of their calls to other species. It also has a relatively low capture rate in mist netting surveys along the LCR (Calvert 2015); however, the species appears to be fairly common at several roost sites in the vicinity of the LCR (Brown 2010). The difficulty in remotely detecting this species using acoustic surveys and mist netting precludes using classic mark-recapture or telemetry techniques to understand even basic demographics of the population along the LCR, in particular those subsets of the population using LCR MSCP restoration sites.

New molecular techniques for estimating population demographics, such as movements, current and historic effective population size (Lande and Barrowclough 1987), and site fidelity, are opening the doors for studying the natural history of rare and elusive species (for a review, see Waits and Paetkau 2005). Historically, the mitochondrial cytochrome *b* gene has proven effective for identifying deep divergences in mammals and other taxa (Bradley and Baker 2001) and has been used as a preliminary marker to identify any deep genetic structuring in California leaf-nosed bat populations in this study.

In addition to mitochondrial deoxyribonucleic acid (mtDNA) analysis, nuclear microsatellites are proving to be a relatively inexpensive yet effective method for identifying population structure and gene flow in both a historic and contemporary context (Hoshino et al. 2012; Paetkau et al. 1995). Due to the stochastic nature of genetic drift, recombination, and differences in selective pressures across the genome, the use of multiple markers is necessary to provide an accurate dataset for microsatellite analyses (Selkoe and Toonen 2006). Historically, the development of an informative microsatellite dataset for non-model organisms has proven time intensive and costly, with variable rates of

success in de novo isolation of microsatellites (Meglecz et al. 2004; Zane et al. 2002). However, in recent years, the development of Next-generation sequencing (NGS) techniques has made sequencing whole genomes a viable option for researchers, allowing for the isolation of large numbers of genetic markers (Ekblom and Galindo 2011). In this study, microsatellite-enriched whole genome sequencing following a modified protocol of the methods outlined in Malausa et al. (2011) was utilized to isolate microsatellite loci.

There can be difficulty in detecting population structure in bats capable of dispersing long distances in relatively short periods of time (Burland and Worthington Wilmer 2001). Additionally, the high number of geographic features capable of becoming roosts for the California leaf-nosed bat in the Southwestern United States (http://www.abandonedmines.gov/) can allow the species to be more or less continuously distributed across the landscape, potentially facilitating a high degree of population admixture, leading to weak signals of structuring in highly variable genetic markers. For these reasons, program STRUCTURE (Pritchard et al. 2000) was used to analyze the microsatellite data, grouping individuals based on genotypic clustering algorithms. STRUCTURE utilizes Bayesian clustering algorithms to compute the likelihood a given genotype originated in a population (K), given estimated allele frequencies. This analytical method has advantages over traditional distance-based methods (neighbor joining and clustering), which are heavily dependent on the chosen distance measure and graphical representation, and are difficult to incorporate confidence measures (Pritchard et al. 2010).

Though STRUCTURE is useful for identifying groups of individuals in weakly divergent data, it assumes the presence of Hardy-Weinberg/linkage populations and may identify the incorrect number of genetic clusters when this assumption is not met, especially for small sample sizes and a limited set of genetic markers (Kalinowski 2011). Discriminant Analysis of Principal Components (DAPC) is a relatively new analytical procedure for identifying and describing genetic clusters that does not assume Hardy-Weinberg populations. DAPC was therefore applied to microsatellite data using the *adegenet* (v. 2.1.1) package of Microsoft Open R (v. 3.5.1) to compare results with those from the STRUCTURE analysis (Jombart et al. 2010). DAPC maximizes between-group variation while minimizing within-group variation. It is far less computationally intensive than Bayesian clustering techniques such as STRUCTURE. DAPC requires an *a priori* definition of the number of groups.

Traditionally, Wright's F statistics (Wright 1965) have been a valuable tool in estimating the reduction in heterozygosity due to genetic structuring. The fixation index (F_{st}) was estimated between and within populations in the study area for both sets of genetic markers. F_{st} ranges from 0, which indicates no population structuring, to 1, the complete fixation of alternate alleles between populations. Average pairwise distances, as well as Nei's distance (Nei 1972), an estimate of average gene diversity per locus useful for closely related populations, were also

calculated as indicators of genetic differentiation among and within populations. A hierarchical analysis of molecular variance (AMOVA) (Excoffier et al. 1992) was run for both datasets, calculating the degree of observed variation among hypothesized groups (F_{ct}), among populations within groups (F_{sc}), and among groups (F_{st}).

Populations that have undergone demographic expansion leave signatures of expansion in their genetic code. These signatures can be evaluated via the comparison of pairwise differences among samples, known as a mismatch distribution (Slatkin and Hudson 1991). A population that has remained stable over long periods of time will naturally accrue a number of mutations, exhibiting a "ragged" multimodal mismatch distribution (Harpending 1994). Contrastingly, a population that has recently undergone a demographic or range expansion will stochastically lose genetic diversity, exhibiting a smooth, skewed mismatch distribution. Related to the mismatch distribution, the Tajima's neutrality test (Tajima 1989) produces the Tajima's D statistic, a normalized version of the expected amount of heterozygosity in a population (θ) subtracted from the observed heterozygosity (π). A negative Tajima's D value is indicative of recent selective sweep or demographic expansion. Mismatch distributions and Tajima's D values were calculated for the mitochondrial data in this study.

LIFE HISTORY

Distribution

The California leaf-nosed bat occurs from the Southwestern United States (north to southern Nevada, Arizona, and southern California), southward throughout Sonora, Mexico, Baja California Sur, Mexico, and the northern portion of Sinaloa, Mexico (Simmons 2005) (figure 1).

Physical Description and Taxonomic History

The California leaf-nosed bat is the only member of the neotropical family Phyllostomidae in the United States. It is a medium sized bat (total length = 85–108 millimeters [mm]), with pelage basally whitish and distally brownish (Anderson 1969). It is most easily identified by its combination of long (> 25 mm) ears and erect, lanceolate nose leaf (Hoffmeister 1986).

The California leaf-nosed bat was originally designated as a full species (Baird 1858, as cited by Rehn 1904). It was later reclassified as a subspecies of Waterhouse's leaf-nosed bat (*Macrotus waterhousii californicus*) (Anderson 1969). Based on chromosomal differences and cranial morphology, the California leaf-nosed bat regained species status in 1974 (Davis and Baker 1974).

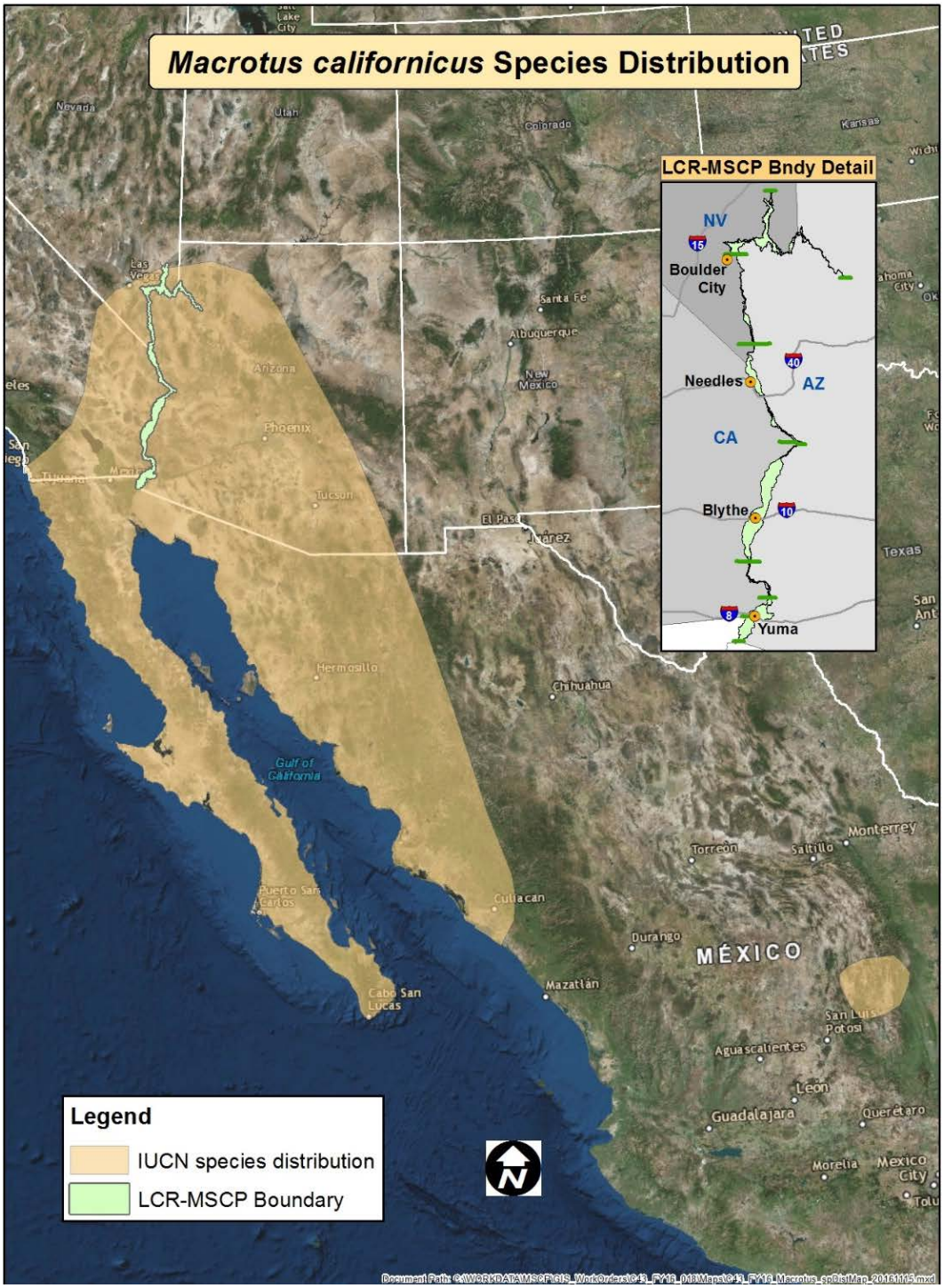

Figure 1.—International Union for the Conservation of Nature distribution map (Solari 2018) for the California leaf-nosed bat.

Habitat, Foraging, and Reproduction

The California leaf-nosed bat is generally regarded as non-migratory. However, Bradshaw noted in his 1961 dissertation a large influx of California leaf-nosed bats during November near Silverbell, Arizona, that he interpreted as a migration event (Bradshaw 1961). The California leaf-nosed bat is a colonial, cave-roosting bat. Roosts are found below 915 meters elevation in caves, mines, and crevices adjacent to desert scrub and riparian habitat. The bats are present year round in the northern portion of their distribution, where they utilize geothermally heated winter roost sites with a stable temperature of 29 degrees Celsius (°C) (Bell et al. 1986). Nightly outflights occur at dusk, and the bats forage by gleaning insects from vegetation in desert scrub and riparian habitats before returning to their roosts. The bats remain active year round and modulate their foraging time according to ambient temperatures (Brown 2011, personal communication). Their prey base includes short-eared and long-eared grasshoppers, long-horned beetles, cicadas, sphinx moths, and noctuid and cossid moths (Hoffmeister 1986).

While the bats do not exhibit migratory behavior, seasonal movements coinciding with reproduction occur. During spring, populations congregate in breeding areas. During summer, females segregate into maternity colonies and males into bachelor colonies. During the fall mating season, males exhibit courtship displays in the maternity roosts (Berry and Brown 1995). While this behavior is similar to lekking observed in other species, the California leaf-nosed bat does not possess a classic lek mating system (Murray et al. 2008). The species exhibits delayed fetal development, and birth of one to two young per year occurs in June (Bradshaw 1962). The young are nursed for a month in nursery colonies until they can fly and forage (Arizona Game and Fish Department 2014).

Conservation Status

The California leaf-nosed bat is not listed as threatened or endangered by the U.S. Fish and Wildlife Service (Environmental Conservation Online System 2016). Under the International Union for the Conservation of Nature Redlist (IUCN), the species is listed as a species of least concern (IUCN 2016). It is listed a species of special concern by the Bureau of Land Management in the States of Arizona, California, and Nevada (Bureau of Land Management 2014, 2017a, 2017b). It is listed as vulnerable by the California Department of Fish and Wildlife (2016) and Arizona Department of Game and Fish (Arizona Game and Fish Department 2012). The primary threats to the species include range contraction due to human disturbance of roosts and loss of foraging habitat (Pierson and Rainey 1998).

METHODS

Sample Collection and Sequencing

Bats were mist netted both at roosts and in foraging areas situated close to their roosts throughout their range (figure 2). Where sampling was not feasible, museum specimens were obtained. Upon capture, a 3-mm wing biopsy punch was taken and stored in a 2 milliliter tube filled with ethanol.

Tissues were extracted using a DNeasy kit (Qiagen Inc, Germantown, Maryland). Extracted deoxyribonucleic acid (DNA) was prepared with two previously described mtDNA cytochrome *b* primers developed for the Waterhouse's leaf-nosed bat (*Macrotus waterhousii*) (Hoffman and Baker 2001) and amplified through a polymerase chain reaction (PCR) at 95 °C for 45 seconds, an annealing temperature of 53 °C for 45 seconds, and an extension at 60 °C for 45 seconds at 34 cycles each. The PCR product was cleaned and run through an ABI 3130 automated sequencer (Applied Biosystems, Foster City, California), checked for ambiguous base calls in Sequencher 4.8 (Gene Codes, Inc., Ann Arbor Michigan), and aligned in program MEGA (Tamura et al. 2007).

Microsatellite enriched NGS was carried out on six individuals from across the species' range using an Illumina HiSeq 2000 sequencer (Illumina, Inc., San Diego, California) at the Research and Testing Laboratory (Research and Testing Laboratory, Lubbock, Texas) using methods outlined in Malausa et al. (2011). The resulting sequences were filtered for variability among individuals, type of microsatellite (pure versus compound), read length, and distance of microsatellite from flanking regions. Fluorescently labelled primers were developed by Integrated DNA Technologies (IDT Technologies, Coralville, Iowa) to allow for multiplexed sequencing across the remaining samples. Double-stranded genomic DNA (gDNA) was quantified using Promega QuantiFluor™ dsDNA System (Promega, Inc., Madison Wisconsin) and the Thermo Fluoroskan Ascent Fluorometer. The gDNA was then normalized to 5 nanograms per microliter (µL). All forward primers were labelled with a fluorescent tag (6FAM, NED, VIC, or PET) attached to the 5 prime end. Multiplexed PCR was run with seven tagged primer sets using the Qiagen Multiplex PCR mix (1X final concentration; Qiagen, Inc., Germantown Maryland) and 20 nanograms of DNA. PCR cycling parameters included a 15-minute hot start at 95 °C, followed by 40 cycles of 95 °C for 30 seconds, an annealing temperature of 53.5 °C for 30 seconds, and an extension at 72 °C for 45 seconds, with a final cycle of 72 °C for 30 minutes. The PCR products were diluted to an appropriate concentration determined by dilution tests. One microliter of diluted PCR product was added to 10 µl of highly deionized Formamide (ThermoFisher, Inc., Waltham, Massachusetts) with the 500 LIZ® size standard (Applied Biosystems, Foster City, California) and 7 µL of molecular grade water. Samples were analyzed on

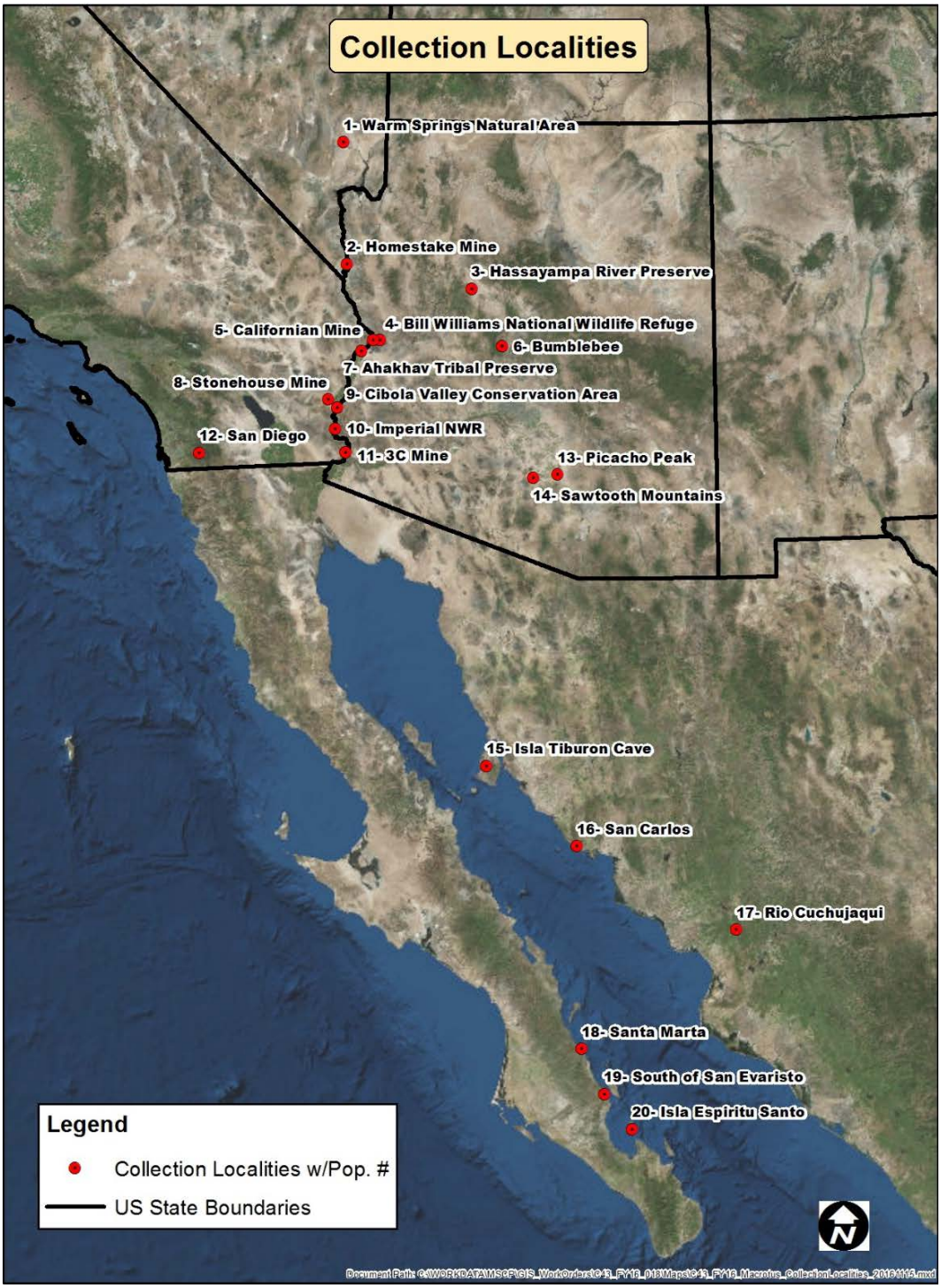

Figure 2.—Sample localities of the California leaf-nosed bat.

an ABI Prism 3730 DNA Analyzer. Sample normalization, PCR, and ABI Prism 3730 DNA analyses were performed at the University of Nevada, Nevada Genomics Center (http://www.ag.unr.edu/ genomics/).

Genetic Analyses

The microsatellite dataset was checked for evidence of null alleles in program Microchecker (Van Oosterhout et al. 2004). The number of alleles, expected and observed heterozygosity, and chi-square tests for deviation from Hardy-Weinberg equilibrium were calculated for the microsatellite dataset using GenAlEx 6.5 (Peakall and Smouse 2012). Allelic and haplotypic diversity, as well as expected and observed heterozygosity, were calculated in DnaSP 6 (Rozas et al. 2017). Pairwise F_{st} values, average pairwise differences, and Nei's distance were generated in Arlequin version 3.5.2.2 (Excoffier et al. 2005) across 17 sampling localities for mitochondrial data and 19 sampling localities for microsatellite data. An AMOVA was conducted on mitochondrial data in Arlequin version 3.5.2.2 for 17 localities using 50,000 permutations and pairwise distance as the molecular distance method. An AMOVA was conducted on the microsatellite data using 50,000 permutations and F-statistics on haplotype frequencies as the molecular distance method. In both AMOVAs, the F_{ct} statistic was calculated for three hypothesized groupings: United States; Sonora, Mexico; and Baja California Sur, Mexico. Haplotype maps were created in ArcGIS (Environmental Systems Research Institute 2011).

Mismatch distributions were generated from the mitochondrial data in Arlequin version 3.5.2.2 using pairwise difference as the molecular distance and 10,000 bootstrap replicates. Tajima's test of neutrality was run for the mitochondrial data in Arlequin version 3.5.2.2 using pairwise difference as the distance method. Both Tajima's D statistic and the mismatch distributions were generated for samples from the United States (n = 76), as well as samples from Sonora, Mexico, and Baja California Sur, Mexico (n = 23). To provide a visualization of the mitochondrial haplotypes, their relative abundance, and connections to other haplotypes, a median joining network was generated using program PopART (Leigh and Bryant 2015).

To determine the most likely number of genetic clusters from the microsatellite data, STRUCTURE was run for 20 independent iterations for K = 1 to K = 20 hypothesized groups with a 50,000-step burn-in period and 50,000 Markov chain Monte Carlo repetitions. Mean estimates of natural logarithm probabilities for groups K = 1 to K = 20 were summarized utilizing STRUCTURE Harvester (Earl and von Holdt 2012).

The *find.clusters* function of *adegenet* was used to sequentially run *k*-means cluster analyses on the data for two to the maximum number of groups assumed for the data (*k*) groups. *Find.clusters* applies the principal component (PC)

analysis to the raw data to obtain a set of independent variables for the cluster analysis. The optimal number of clusters is chosen according to Bayesian information criterion (BIC) (i.e., the number of groups for which BIC is smallest). Discriminant analysis is then performed on the PCs to assign individual samples to clusters. The *optim.a.score* function was used to identify the optimal number of PCs to retain for discriminant analysis based on the difference between the proportion of successful reassignments of observed versus random groups (Jombart and Collins 2017), which suggested four PCs were appropriate for the microsatellite data. Scatterplots and STRUCTURE type plots were generated to visually assess whether group assignment of samples indicated any geographical pattern in genetic clustering (e.g., whether sample sites were grouped according to distances among sites). The latter were generated with the *compoplot* function of *adegenet*. Scatterplots with inertia ellipses were created using the R package *ggplot2* to mimic and annotate the default plots generated by the *scatterplot* function in *adegenet.* Inertia ellipses are graphical summaries of the PC coordinates for the individuals within each cluster. The degree of overlap represents how well groups are differentiated. The center of the ellipse equals the mean of the coordinates, and the horizontal and vertical widths are equal to their variances. The slope is determined by their covariance. Inertia ellipses are equal to a confidence ellipse only for data following a bivariate normal distribution, in which case the default level is equal to 0.67. Ellipses were created with *ggplot2* using a confidence level of 0.63 to mimic the inertia ellipses generated by the function in *adegenet*, but they do not represent true confidence ellipses.

RESULTS

Sequencing

Mitochondrial sequencing resulted in 916 base pairs of the cytochrome *b* gene. Analysis revealed 18 total haplotypes in 91 samples from 17 localities across the range and 5 haplotypes present within 8 localities from the LCR region, 3 of which were found nowhere else in the range (figure 3 and table 1). Haplotype 1 is common and broadly distributed across the LCR and adjacent survey sites in the Southwestern United States. Haplotype 2 was detected in bats collected from the Californian, Stonehouse, and 3C Mines as well as the Imperial National Wildlife Refuge. Haplotype 3 was only detected in the Californian Mine. Haplotype 6 was detected in the 3C and Stonehouse Mines as well as the Cibola Valley Conservation Area. Haplotypes 4 and 5 were present in the Sonoran portion of the range as well as the Southwestern United States.

Microsatellite enriched NGS produced hundreds to thousands of microsatellite loci for each sample (table 2). Of 60 selected microsatellites, 6 were successfully amplified, sequenced, and visually screened for variability in Sequencher 4.8 (Gene Codes, Inc., Ann Arbor Michigan). Sequencing conducted at the University of Nevada, Reno Genomics Center, resulted in six microsatellite loci.

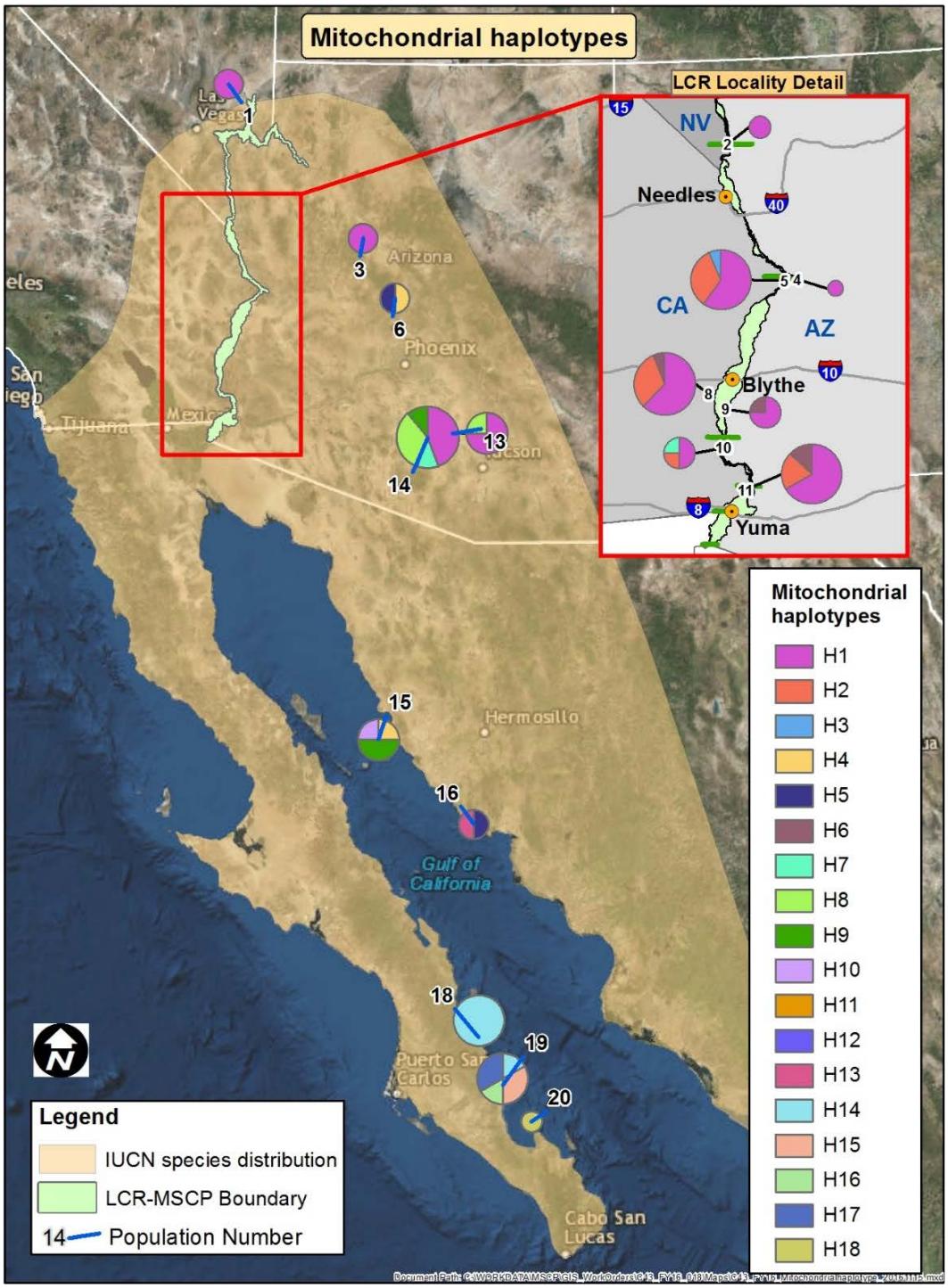

Figure 3.—Mitochondrial haplotype map.

Table 1.—Mitochondrial haplotype list

Locality	Population #	Number of samples	H1	H2	H3	H4	H5	H6	H7	H8	H9	H10	H11	H12	H13	H14	H15	H16	H17	H18
Warm Springs Natural Area	1	2	2	0	0	0	0	0	0	0	0	0	0	0	0	0	0	0	0	0
Homestake Mine	2	2	2	0	0	0	0	0	0	0	0	0	0	0	0	0	0	0	0	0
Hassayampa Preserve	3	2	2	0	0	0	0	0	0	0	0	0	0	0	0	0	0	0	0	0
Bill Williams National Wildlife Refuge	4	1	1	0	0	0	0	0	0	0	0	0	0	0	0	0	0	0	0	0
Californian Mine	5	15	9	5	0	0	0	0	0	0	0	0	0	0	0	0	0	0	1	0
Bumblebee	6	2	0	0	0	0	0	0	1	1	0	0	0	0	0	0	0	0	0	0
Stonehouse Mine	8	16	10	5	0	0	0	0	0	0	0	0	0	0	0	0	0	0	0	1
Cibola Valley Conservation Area	9	4	3	0	0	0	0	0	0	0	0	0	0	0	0	0	0	0	0	1
Imperial National Wildlife Refuge	10	4	2	1	1	0	0	0	0	0	0	0	0	0	0	0	0	0	0	0
3C Mine	11	15	10	3	0	0	0	0	0	0	0	0	0	0	0	0	0	0	0	2
Picacho Peak	13	5	3	0	0	1	1	0	0	0	0	0	0	0	0	0	0	0	0	0
Sawtooth Mountains	14	11	6	0	1	3	1	0	0	0	0	0	0	0	0	0	0	0	0	0
Isla Tiburon Cave	15	4	0	0	0	0	0	0	0	1	0	0	0	2	1	0	0	0	0	0
San Carlos	16	6	0	0	0	0	0	0	0	1	0	1	4	0	0	0	0	0	0	0
Santa Marta	18	6	0	0	0	0	0	0	0	0	6	0	0	0	0	0	0	0	0	0
San Evaristo	19	6	0	0	0	0	0	0	0	0	1	0	0	0	0	2	1	2	0	0
Isla Espiritu Santo	20	1	0	0	0	0	0	1	0	0	0	0	0	0	0	0	0	0	0	0

Table 2.—Whole genome sequencing results for six individuals

Sample name	Validated loci	Percent loci identified from several sequences	Perfect microsatellites	Compound microsatellites
LVT2433	4,661	23	2,094	455
LVT4992	5,163	28	2,225	509
LVT10055	1,544	30	593	139
LVT10057	2,147	25	888	193
NK11120	3,274	27	1,403	336
NK80553	2,696	25	1,052	269

Genetic Analyses

Evidence of one microsatellite null allele was found in Micro-Checker and was removed from analyses, resulting in five usable loci (table 3). Due to a low sample size for many populations, within-population statistics were difficult to calculate across sampling localities.

Table 3.—Microsatellites and associated primer information

Primer forward/reverse	Forward	Reverse	Product size	Repeat motif	Tag	Tm by multiplex	Range
MCMSL33/R33	GTT TGT GGT GAC AGT GTG GC	AGT CCT TCC TCT GTG CAC AC	214	(GT)	**6-FAM**	65.08	184–234
MCMSL35/R35	CCT CAG AAC AGG CAC CCA TC	GTC GCT CCC TTC GAA TCT GA	144	(CA)	**VIC**	63.9	124–164
MCMSL5/R5	AGG AGA GTG AAT CCC TAT ATC AGC	CTG CCA AGG GAA CTG CCT TT	298	(CAA)	**VIC**	63.87	278–318
MCMSL6/R6	TTT GCA AAC CGT TTA TCT GAT AAA C	GCC TTT GTG CAT GCT CAG TG	205	(ATC)	**PET**	60.63	185–225
MCMSL60/R60	GTC CAC CTC TAC CTC CCA CT	ACT GTC AAA GGG TAG TGG GT	198	(AGAT)	**VIC**	63.66	178–218

Deviation from Hardy-Weinberg equilibrium was tested for microsatellite samples. Out of the dataset, seven samples had significant values, indicating they were not in Hardy-Weinberg equilibrium (table 4). Microsatellite summary statistics revealed a small number of alleles per locus and generally higher than expected heterozygosity. The full table of values is located in attachment 1 (table 1-3).

Table 4.—Summary of chi-square test of Hardy-Weinberg equilibrium

Summary of chi-square tests for Hardy-Weinberg equilibrium					
Loci	5				
Samples	88				
Populations	20				
Population	**Locus**	**Degrees of freedom**	**Chi-squared value**	**P-value**	**Significant**
Stonehouse Mine	Locus5	15	33.535	0.004	P < 0.01
3C Mine	Locus4	3	11.484	0.009	P < 0.01
3C Mine	Locus5	21	44.171	0.002	P < 0.01
Sawtooth Mountains	Locus4	1	4.000	0.046	P < 0.05
Isla Tiburon Cave	Locus1	3	10.000	0.019	P < 0.05
Isla Tiburon Cave	Locus4	1	5.000	0.025	P < 0.05
South of San Evaristo	Locus5	6	21.000	0.002	P < 0.01

Pooled sequence statistics of 917 base pairs across 102 sequences showed 25 variable sites and a relatively low nucleotide diversity (Pi = 0.00206) (table 5). When broken up into sequences from the United States (n = 80) and Baja California Sur plus Sonora, Mexico (n = 22), the northern samples have a relatively lower nucleotide diversity (Pi = 0.00135 for northern samples versus 0.00366 southern samples) and haplotype diversity (Northern Hd = 0.579 versus Southern Hd = 0.866) (tables 6 and 7). The median joining network showed one commonly occurring haplotype present in samples from the United States, and one haplotype shared between Sonoran samples and one sample in Arizona (figure 4). There were no shared haplotypes between Baja California Sur, Mexico, and any other locality. The median joining network data table showing membership of each node is in attachment 1 (table 1-2).

Mitochondrial AMOVA analysis reported 47.90% of the observed variation being attributed to among group differences, (F_{ct} = 0.47902, P = 0.00153), 5.99% attributed to differences among populations within groups (F_{sc} = 0.11499, P = 0.02029) and 46.11% attributed to differences among populations (F_{st} = 0.53892, P = 0.00000) (table 8).

Table 5.—Mitochondrial pooled sequence statistics

Number of variable sites, S: 25
Total number of mutations, Eta: 25
Nucleotide diversity (per site), Pi: 0.00206
Sampling variance of Pi: 0.0000001
Standard deviation of Pi: 0.00025
Average number of nucleotide differences, k: 1.89342
Theta (per sequence) from S, Theta-W: 4.81021
Theta (per site) from S, Theta-W: 0.00525
Number of haplotypes, h: 18
Haplotype (gene) diversity, Hd: 0.735
Variance of haplotype diversity: 0.00187
Standard deviation of haplotype diversity: 0.043

Table 6.—Sequence statistics for northern range samples

Number of variable sites, S: 15
Total number of mutations, Eta: 15
Nucleotide diversity (per site), Pi: 0.00135
Average number of nucleotide differences, k: 1.23924
Number of haplotypes, h: 10
Haplotype (gene) diversity, Hd: 0.579
Variance of haplotype diversity: 0.00336
Standard deviation of haplotype diversity: 0.058

Table 7.—Sequence statistics for southern range samples

Number of variable sites, S: 15
Total number of mutations, Eta: 15
Nucleotide diversity (per site), Pi: 0.00366
Average number of nucleotide differences, k: 3.35498
Number of haplotypes, h: 9
Haplotype (gene) diversity, Hd: 0.866
Variance of haplotype diversity: 0.00259
Standard deviation of haplotype diversity: 0.051

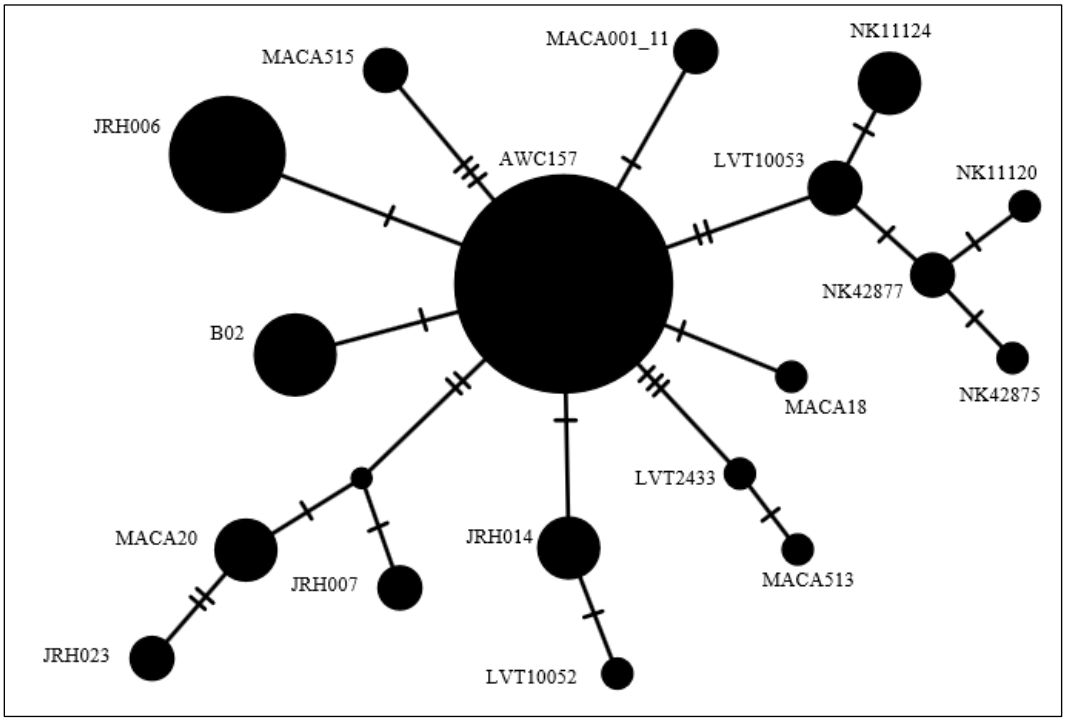

Figure 4.—Mitochondrial median joining network.
Hash marks are base pair changes between nodes.

Table 8.—Mitochondrial AMOVA results

MtDNA
Distance method: Pairwise difference

Source of variation	Degrees of freedom	Sum of squares	Variance components	Percentage of variation
Among groups	2	27.094	0.65094 Va	47.90
Among populations within groups	14	15.266	0.08141 Vb	5.99
Within populations	85	53.258	0.62656 Vc	44.11
Total	**101**	**95.618**	**1.35890**	

Fixation indices

F_{sc}: 0.11499
F_{st}: 0.53892
F_{ct}: 0.47902

Significance tests (50,175 permutations)

V_c and F_{st}: P (random value < observed value) = 0.00000
P (random value = observed value) = 0.00000
P-value = 0.00000 + -0.00000

V_b and F_{sc}: P (random value > observed value) = 0.02029
P (random value = observed value) = 0.00000
P-value = 0.02029 + -0.00057

V_a and F_{ct}: P (random value > observed value) = 0.00153
P (random value = observed value) = 0.00000
P-value = 0.00153+-0.0001

Microsatellite AMOVA analysis reported 0.06% of the observed variation attributed to among group differences (F_{ct} = 0.00059, P = 0.18906), 0.33% attributed to differences among populations within groups (F_{sc} = 0.00327, P = 0.20229), and 99.60% attributed to differences within populations (F_{st} = 0.00445, P = 0.14348) (table 9).

Table 9.—Microsatellite AMOVA results

Microsatellites

Computing conventional F-statistics from haplotype frequencies

Source of variation	Degrees of freedom	Sum of squares	Variance components	Percentage of variation
Among groups	2	1.072	0.00059 Va	0.12
Among populations within groups	17	8.609	0.00162 Vb	0.33
Within populations	154	76.025	0.49367 Vc	99.56
Total	**173**	**85.707**	**0.49588**	

Fixation Indices

F_{sc}: 0.00327

F_{st}: 0.00445

F_{ct}: 0.00118

Significance tests (50,175 permutations)

V_c and F_{st}: P (random value < observed value) = 0.14296

P (random value = observed value) = 0.00052

P-value = 0.14348 + -0.00161

V_b and F_{sc}: P (random value > observed value) = 0.20157

P (random value = observed value) = 0.00072

P-value = 0.20229 + -0.00179

V_a and F_{ct}: P (random value > observed value) = 0.18906

P (random value = observed value) = 0.00000

P-value = 0.18906 + -0.00179

Tajima's D statistic was reported as -1.80324 (P = 0.01096) for all samples (n = 102) (table 10), -1.41551 (P = 0.05756) for samples from the United States (n = 80) (table 11), and -0.50051 (P = 0.34128) for samples from Sonora, Mexico, and Baja California Sur, Mexico (n = 22) (table 12).

Table 10.—Tajima's neutrality test for all samples

Sample size	102
Number of sites with substitutions (S)	25
Mean number of pairwise differences (Pi)	1.89342
Distance method	Pairwise difference
Tajima's D	-1.80324
Number of simulations	50000
Observed theta(S)	4.81021
Mean theta(S)	4.80191
Standard deviation theta(S)	1.52171
Mean D	-0.08829
Standard deviation D	0.91330
P(D simulated < D observed)	0.01096

Table 11.—Tajima's neutrality test for northern range samples

Sample size	80
Number of sites with substitutions (S)	12
Mean number of pairwise differences (Pi)	1.17754
Distance method	Pairwise difference
Tajima's D	-1.41551
Number of simulations	50000
Observed theta(S)	2.42899
Mean theta(S)	2.43155
Standard deviation theta(S)	0.94635
Mean D	-0.06878
Standard deviation D	0.93776
P(D simulated < D observed)	0.05756

Table 12.—Tajima's neutrality test for southern range samples

Sample size	22
Number of sites with substitutions (S)	15
Mean number of pairwise differences (Pi)	3.49407
Distance method	Pairwise difference
Tajima's D	-0.50051
Number of simulations	50000
Observed theta(S)	4.06414
Mean theta(S)	4.06142
Standard deviation theta(S)	1.74413
Mean D	-0.07281
Standard deviation D	0.91775
P(D simulated < D observed)	0.34128

For the mitochondrial data, the pairwise F_{st} matrix (figure 5) and pairwise difference/Nei's distance matrix (figure 6) indicated a higher level of structuring in the samples from Sonora, Mexico, and Baja California Sur, Mexico, relative to the samples from the northern portion of the range.

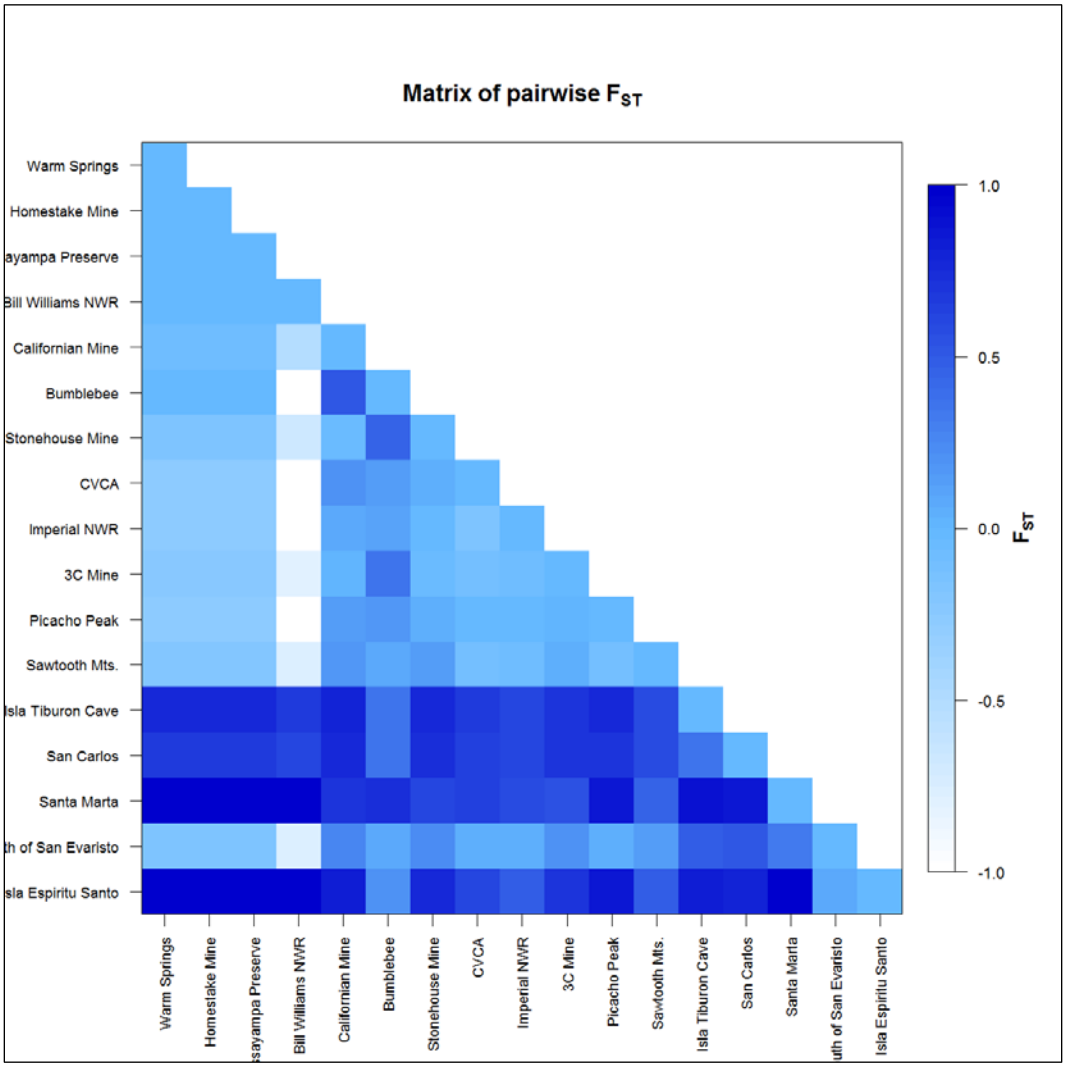

Figure 5.—Matrix of pairwise F_{st} values for mitochondrial data.

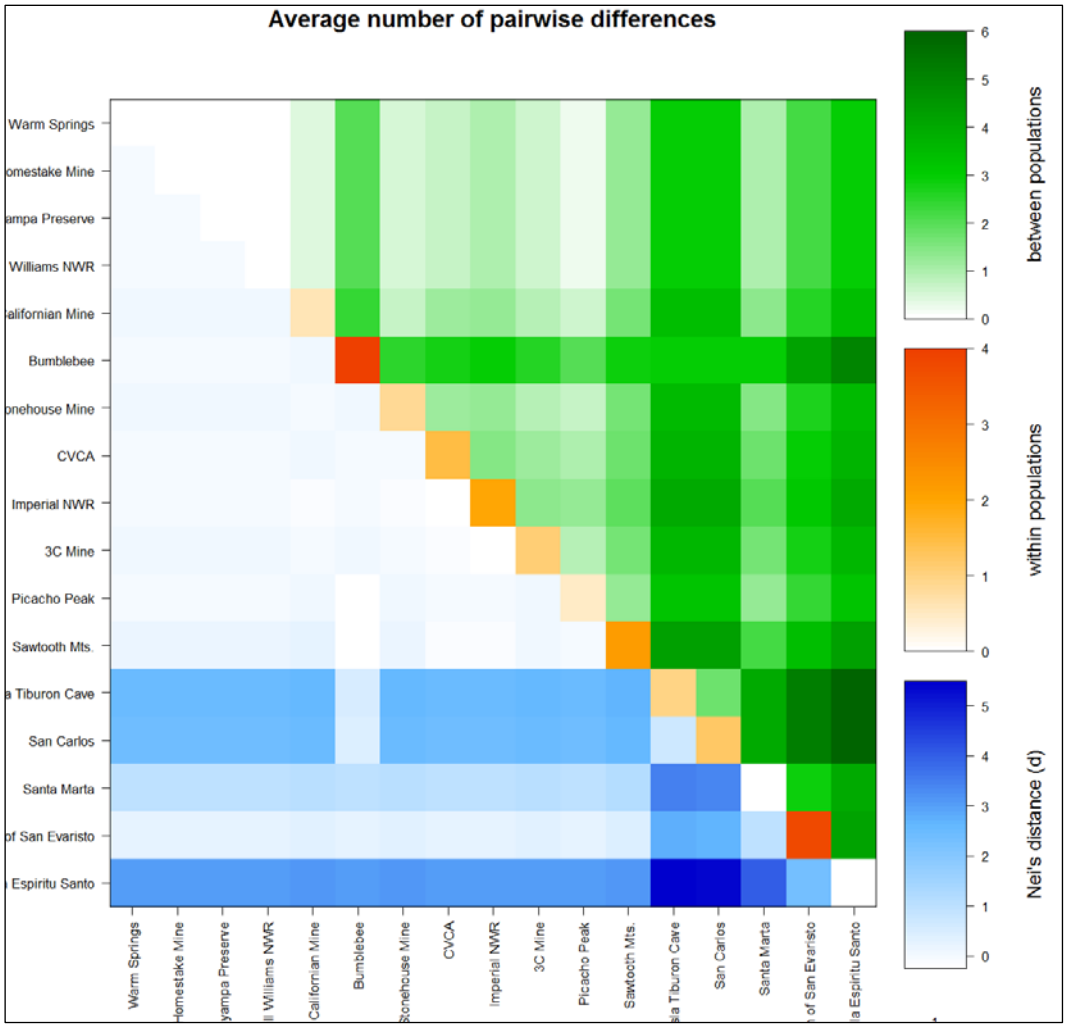

Figure 6.—Matrix of pairwise differences within and between populations, and Nei's distance for mitochondrial data.

A mismatch distribution of the total range exhibited a right-skewed distribution (figure 7). Upon dividing samples into northern and southern range, mismatch distributions showed a relatively lower number of pairwise differences in the samples from the United States (figure 8) as compared to the samples from Sonora, Mexico, and Baja California Sur, Mexico (figure 9).

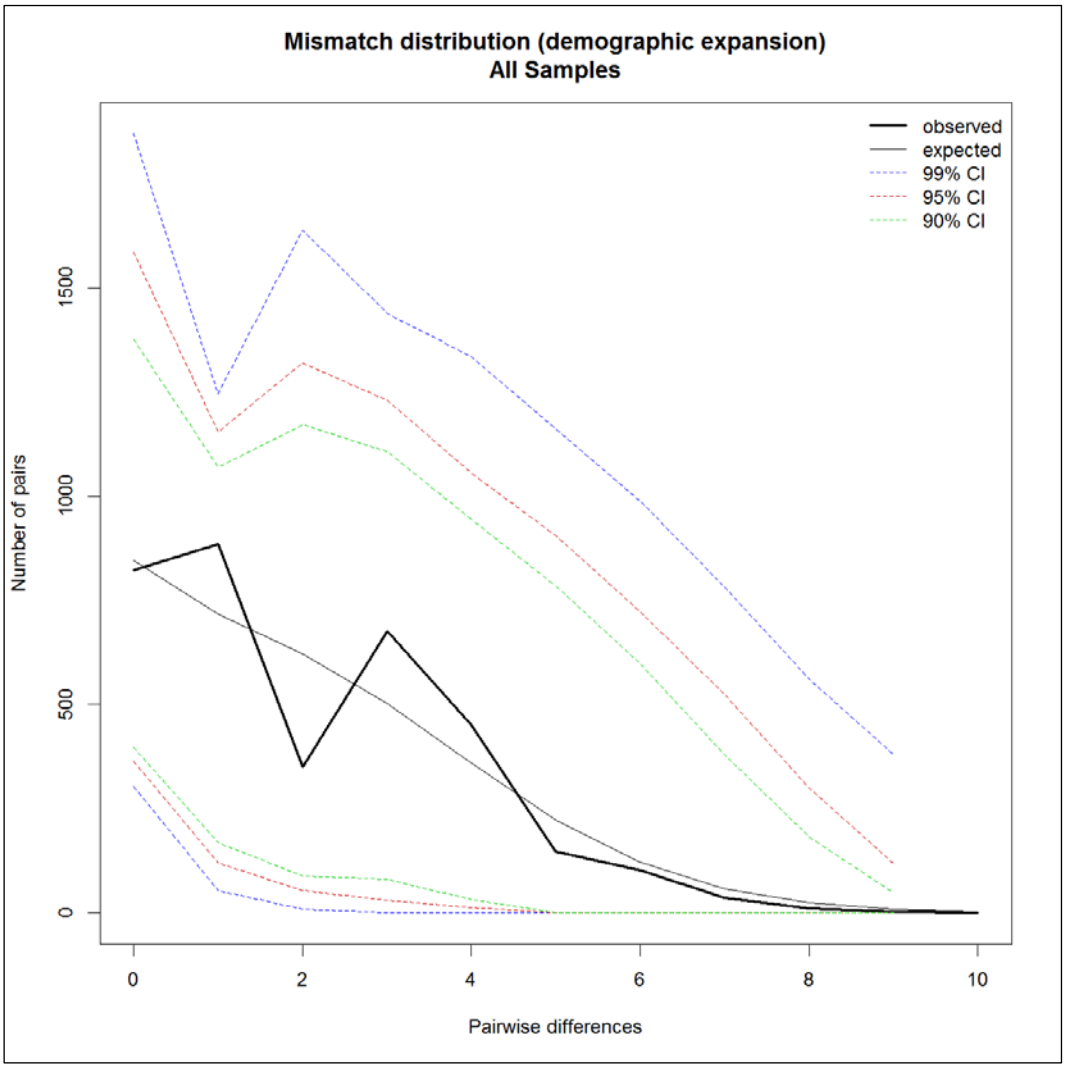

Figure 7.—Mismatch distribution for all mitochondrial samples (n = 99).

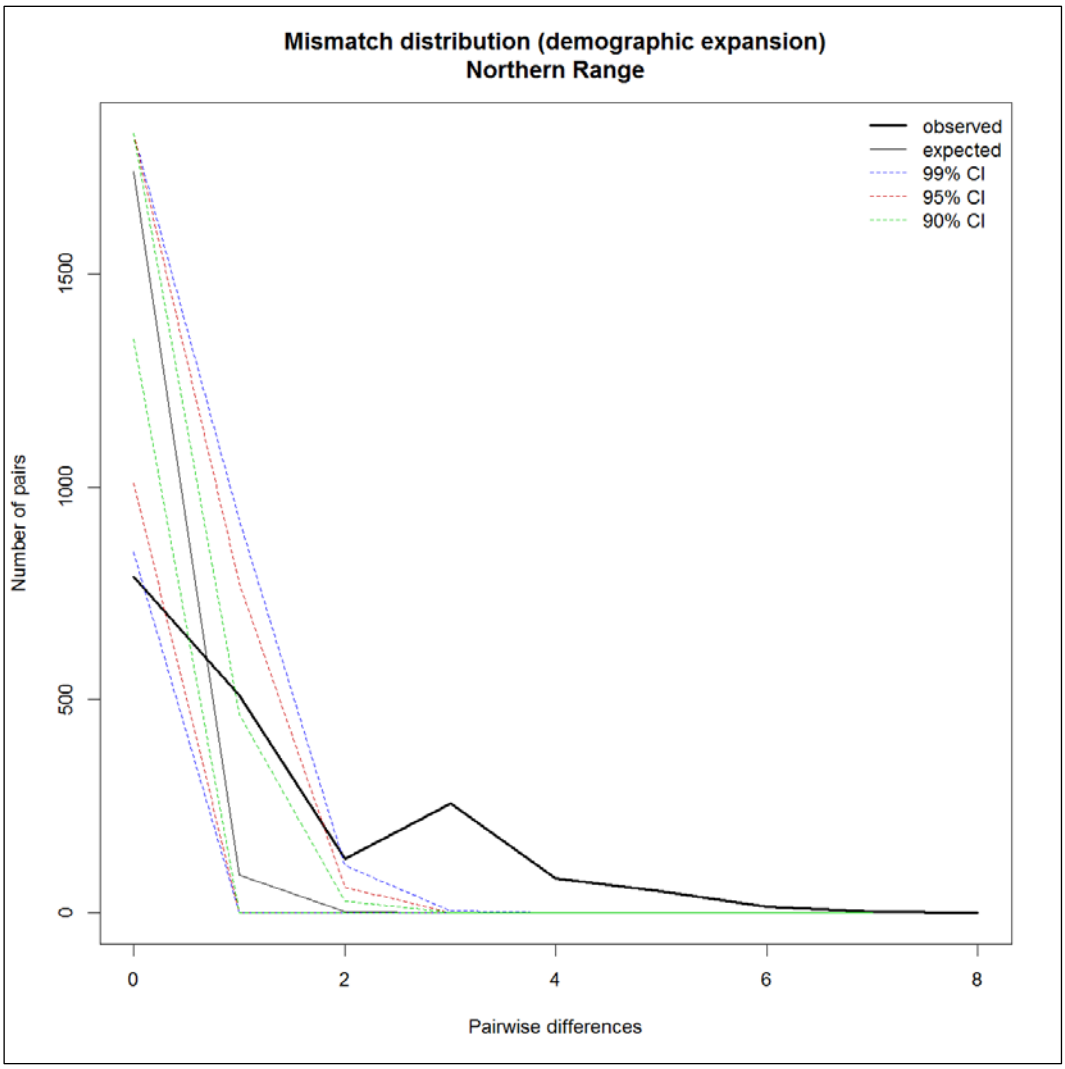

Figure 8.—Mismatch distribution for mitochondrial data from the United States (n = 76).

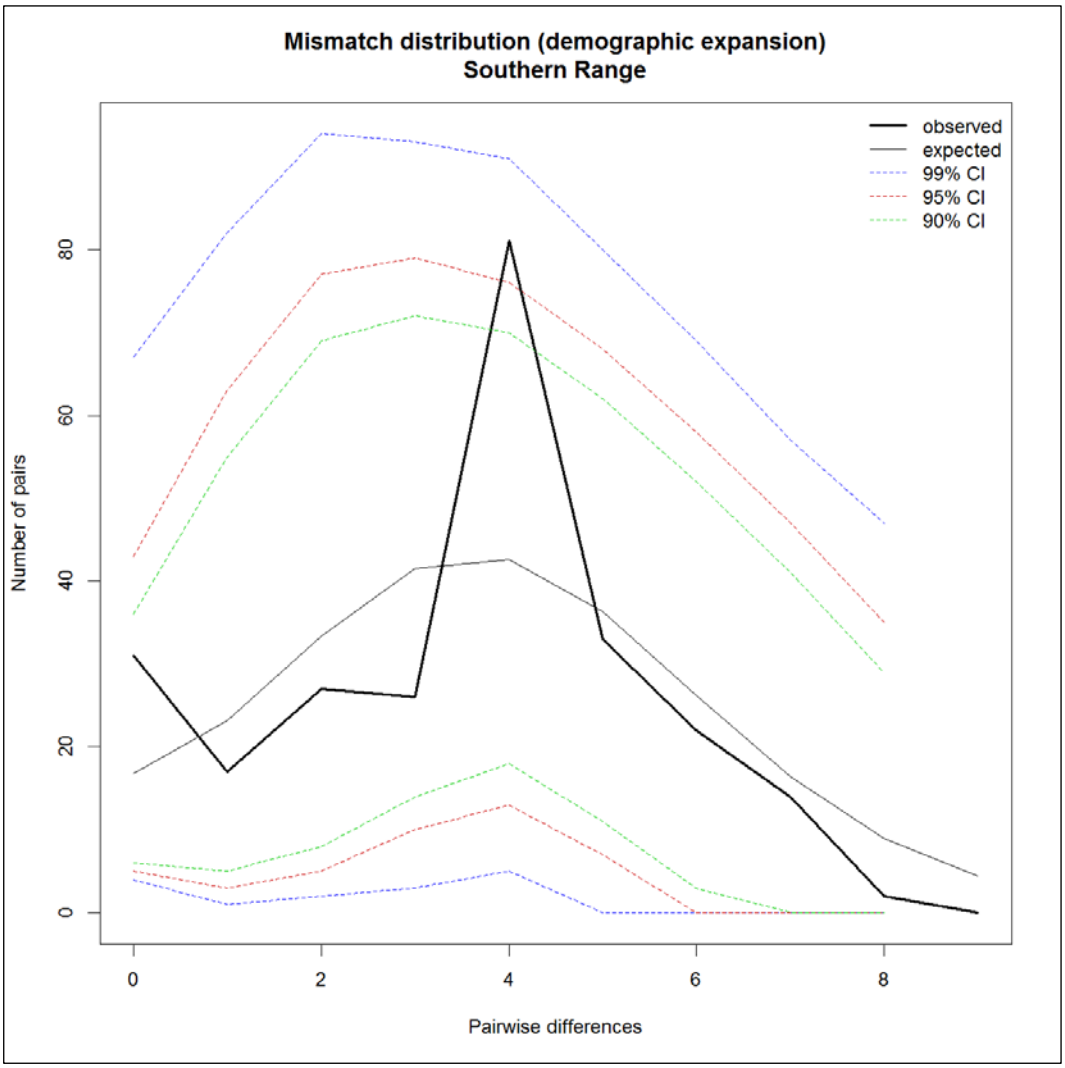

Figure 9.—Mismatch distribution for mitochondrial data from Baja California Sur, Mexico, and Sonora, Mexico (n = 23).

From the 20 independent STRUCTURE runs, K = 3 groups had the most support (figure 10). Though K = 3 was the most supported, K = 2 was selected, as STRUCTURE tends to overestimate the number of clusters (Pritchard et al. 2010). The two groups were distributed across the species' range, with no discernable geographic pattern (figure 11).

Pairwise F_{st} values for the microsatellite data were low across every comparison, except for Rio Cuchujaqui, in Sonora, Mexico (figure 12). A similar pattern was observed for the average pairwise differences/Nei's distance matrix (figure 13).

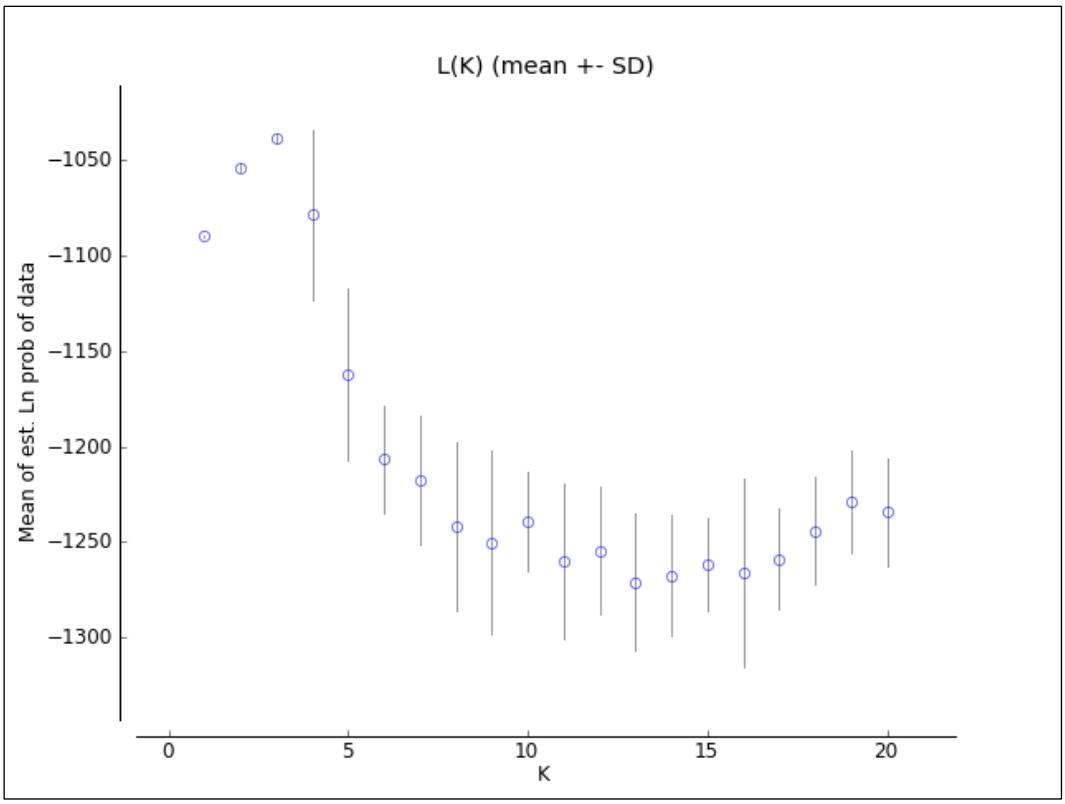

Figure 10.—Mean natural logarithm probability of microsatellite data for K = 1 to K = 20 across 20 runs.

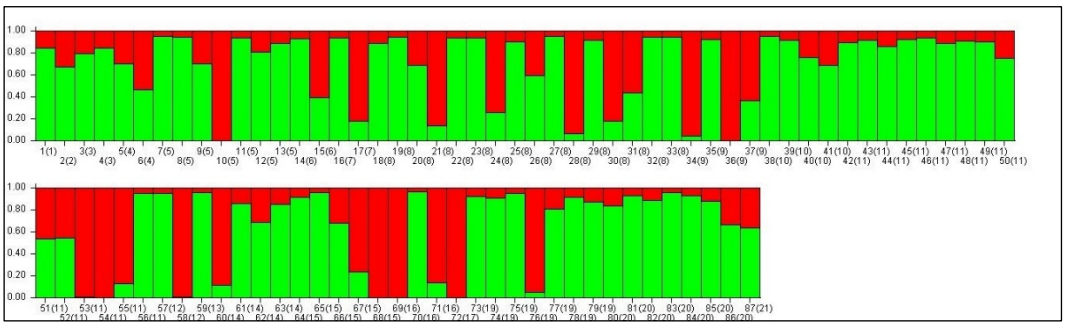

Figure 11.—STRUCTURE results for K = 2 clusters.
Numbers are individuals, and numbers in parentheses are sampling localities. The y-axis is the probability of membership of each individual to either cluster.

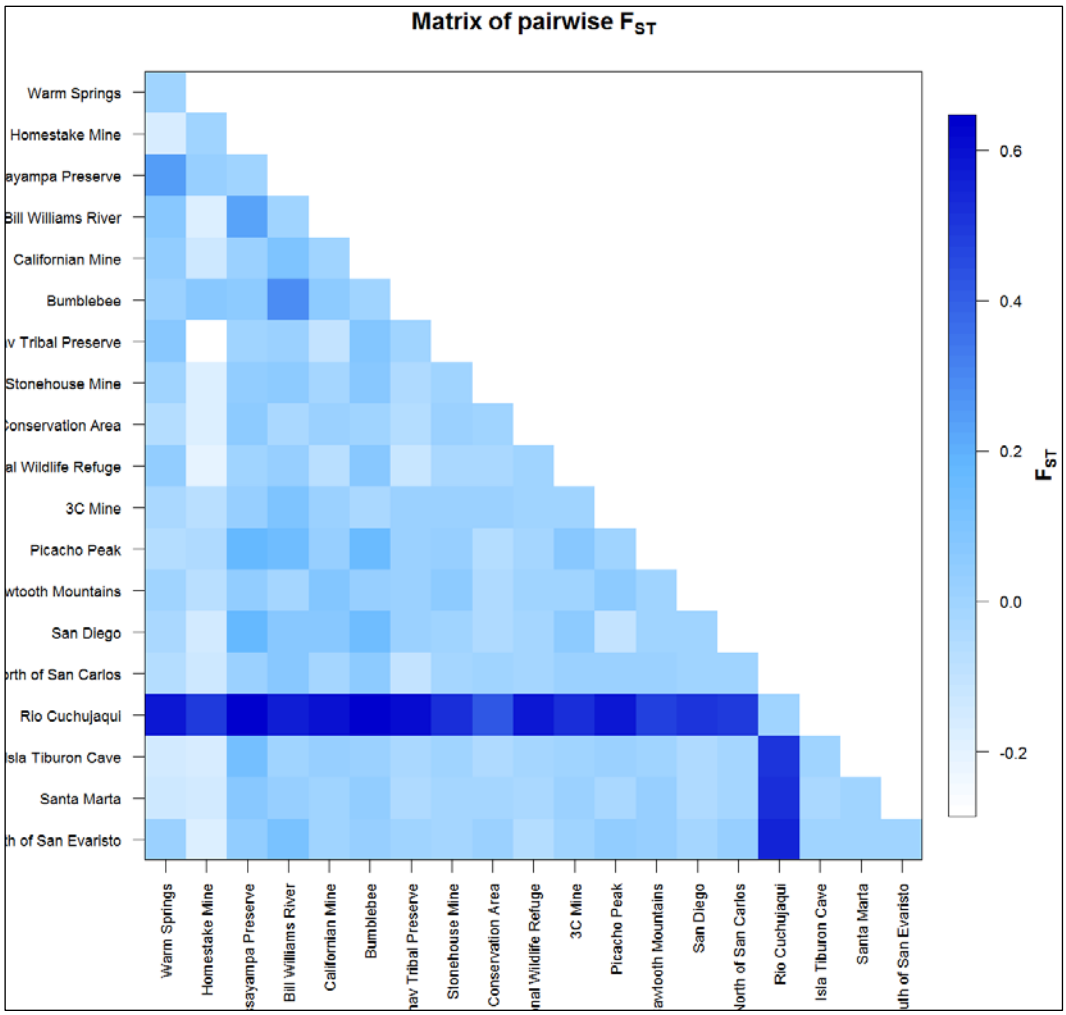

Figure 12.—Matrix of pairwise F_{st} values for microsatellite data.

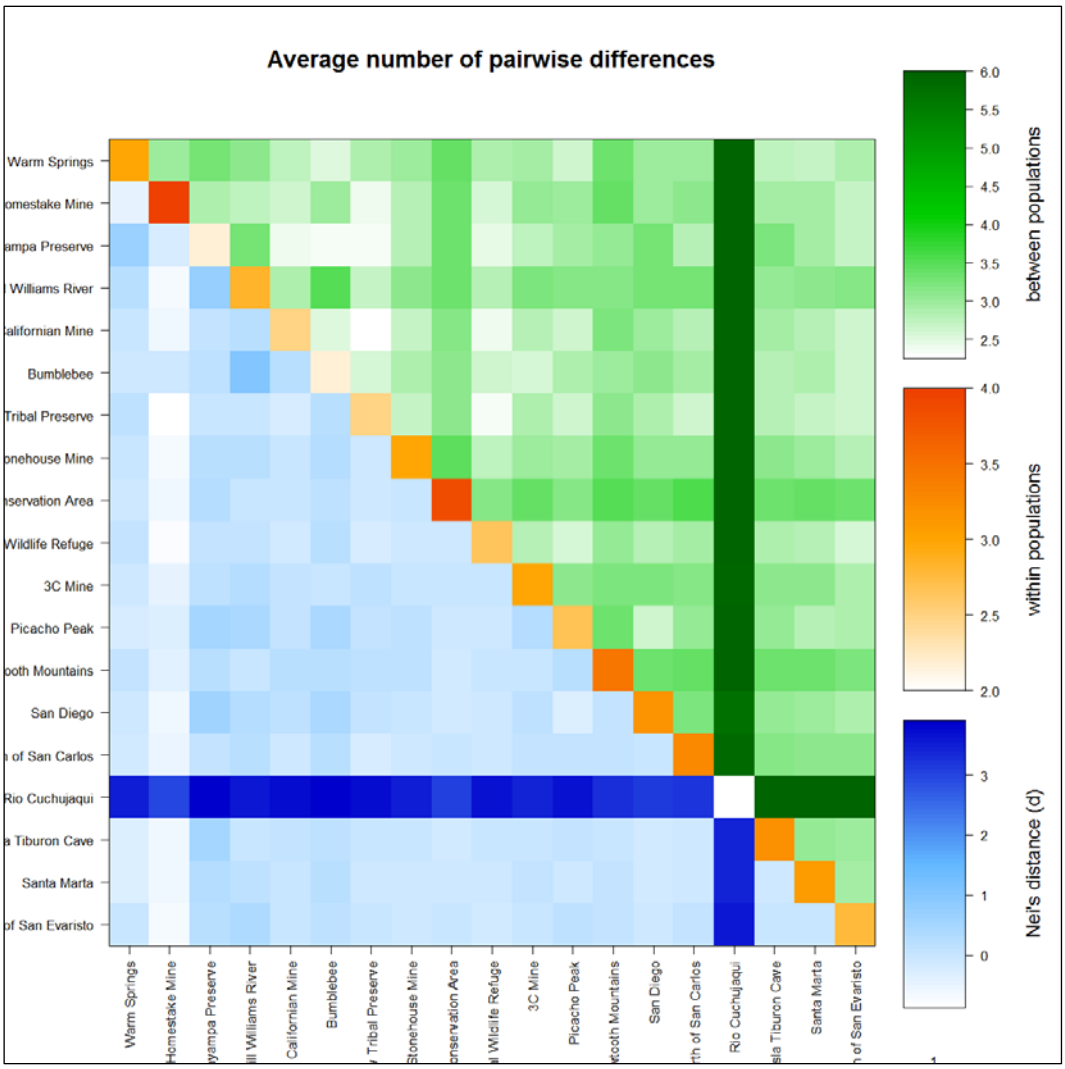

Figure 13.—Matrix of pairwise differences and Nei's distance for microsatellite data.

Four clusters were chosen for DAPC based on the minimum BIC score, and the first four PCs (40% of total variance) were used as recommended by the *optim.a.score* function. A scatterplot of individual scores on the first two PCs, colored by cluster and labeled by sample site, shows a relatively clear distinction among genetic clusters identified by DAPC but no clear geographic pattern related to sample sites (figure 14). The STRUCTURE-type plot reveals admixing (defined as less than 90% probability of membership to a single cluster) for 18 individuals, most of which were from the northern sampling sites (figure 15). Despite differences in the number of identified clusters, DAPC results were qualitatively similar to STRUCTURE results in that there was no clear evidence of a geographic pattern associated with clusters.

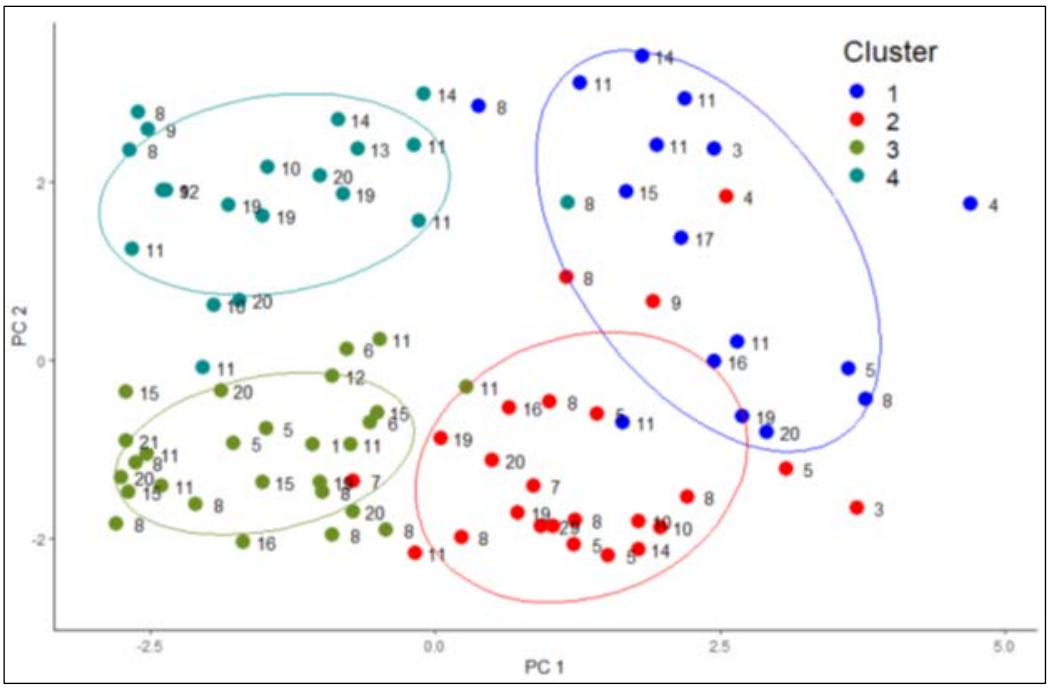

Figure 14.—Scatterplot showing individuals colored by clusters with inertia ellipses (based on four PCs).
Individuals are labeled by sampling site. The inertia ellipse is approximated from normal ellipse with a confidence level of 0.63.

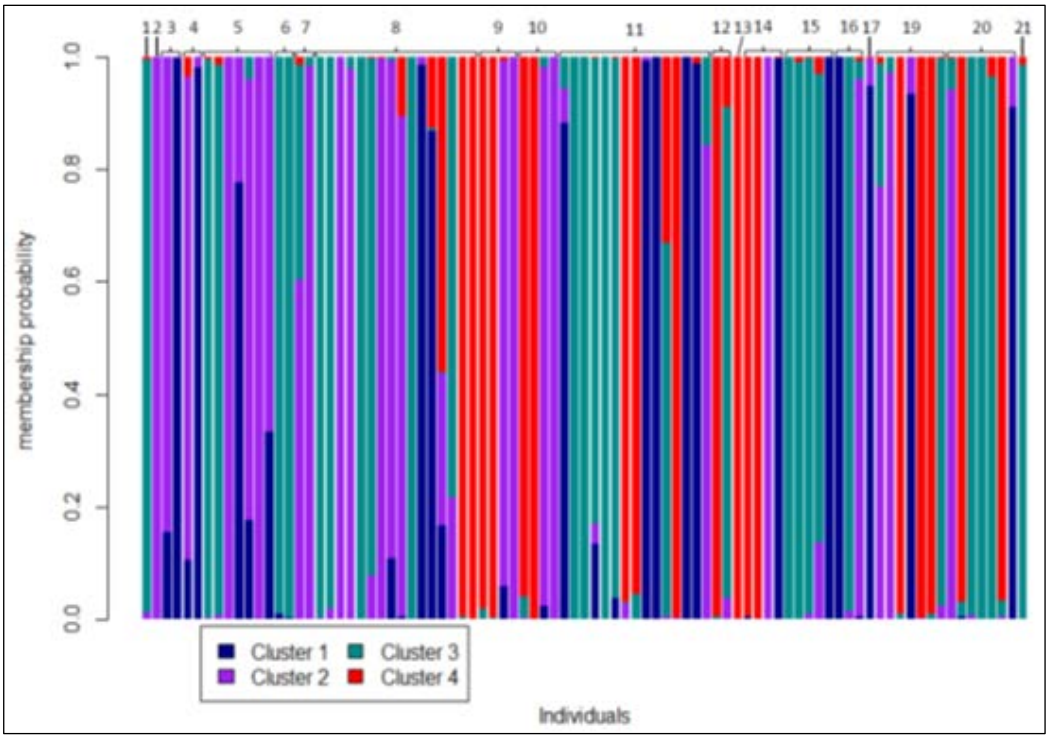

Figure 15.—STRUCTURE type DAPC plot: Individual bars labeled by sample site (four PCs).

DISCUSSION

The first goal of this project was to document genetic structuring of roosts along the LCR and contrast the genetic diversity found within the LCR to that found around the species' range. There has been precedent for this area's importance in other species. The LCR flood plain retained relatively warmer conditions during the last glacial maximum (Thompson and Anderson 2000), and may have served as a refugium for warm-adapted desert species, leading to a high degree of genetic diversity relative to the rest of the home range of similarly distributed mammals (Jezkova et al. 2009). The mitochondrial data have revealed a high haplotype diversity and low nucleotide diversity within the LCR. The network diagram shows only 2 out of 18 haplotypes present across a broad range (AWC157, LVT10053). Within the LCR, there are five haplotypes, with one broadly distributed and three unique to the LCR. Interestingly, the haplotypes found in Baja California Sur, Mexico, were more divergent than those between other sampling locations and were not found in any other localities. Though there has been documented peninsular vicariance for other species due to Pleistocene climatic changes (Riddle et al. 2000), the reason for this genetic discontinuity is unclear without a more robust sampling of the range. While difficult to say with certainty, given the uneven sampling, there seems to exist within the samples a gradient of high diversity to low diversity from the center of the species' range to the northern periphery. Nucleotide diversity and haplotype diversity are higher in the southern samples even with the relatively lower sample size. This is in line with what is seen in other species (Garner et al. 2003; Hutchinson 2003; Schwartz et al. 2003), as the edge of the species' range is presumably less suitable, exacerbating the effects of genetic drift due to a reduced subset of the breeding population. The new world leaf-nosed bats are primarily neotropical species, so the increased genetic diversity closer to the tropics is unsurprising.

The presence of three unique haplotypes in the range has a number of possible reasons. One possibility is that the populations along the LCR may have been isolated for long enough to accrue unique polymorphisms. Another more likely possibility is that these unique haplotypes may be present throughout the range and missed due to the limited sample size from outside of the LCR. The presence of shared haplotypes between northern and southern reaches of the species' range may be due to shared ancestry, as of yet undocumented long-distance migration among populations, or incomplete lineage sorting during genetic analysis. Incomplete lineage sorting creates a discrepancy between gene trees (in this case, cytochrome *b*) and the overall species-level phylogenetic tree due to shared haplotypes being present in recently divergent populations. A solution to the potential for incomplete lineage sorting is to evaluate concordance across a number of markers.

Though K = 3 was slightly more supported in the STRUCTURE analysis, in the case of such closely supported groupings, the conservative estimate is the correct

choice, as STRUCTURE can overestimate K (Pritchard et al. 2010). The microsatellite markers showed a low level of structuring, exhibiting small fixation indices, poor grouping in STRUCTURE, and a majority of the variation explained by within-population differences in AMOVA analyses. Contrasted with the higher degree of structuring observed in the mitochondrial data, this discordance between genomic and maternally inherited markers may reflect a high degree of female philopatry in the California leaf-nosed bat. Philopatry is commonly seen as an optimal life history strategy for female mammals (Clutton-Brock and Lukas 2011), and it is known that maternity colony locations tend to remain in the same locations throughout the years (Brown 2011, personal communication). One reason for the use of microsatellite data was the hope that there would be enough detectable structuring to allow for "fingerprinting" of roosts along the LCR region. The assignment of captured individuals to their roosts through genotype assignment tests would provide valuable information and efficiency to biologists concerned with system-wide monitoring of the species. Based on the low levels of structuring seen in the microsatellite data, this was not found to be possible.

The chi-square tests for microsatellite data indicated that allele frequencies deviated strongly from Hardy-Weinberg equilibrium. Many of the genetic analyses run have Hardy-Weinberg equilibrium as a built-in assumption in their models. The DAPC analysis was run as a supplemental analysis method free of those assumptions. While more clusters were identified with DAPC (4) than STRUCTURE (2), neither analysis revealed any association between clusters and geographic distribution of sample sites.

The second goal of this project was to provide estimates for the current and historic effective population size (N_e) of the LCR population, including the timing of changes in population size. A recent increase in N_e could have implicated the impact of a mining boom in the Southwestern United States on nearby California leaf-nosed bat populations. Estimates of N_e were not obtained within the timeframe of the project. As indicators of demographic expansion, the mismatch distributions and Tajima's D statistic both pointed to a reduced degree of nucleotide diversity within the northern portion of the species' range. The strongly negative Tajima's D values in the pooled statistic, as well as for the northern range, can reflect several scenarios: They could point to a recent range expansion into the north following the opening of available roost habitat. Alternatively, they could result from a recent population bottleneck or population expansion following the last glacial maximum (Grant 2015).

LITERATURE CITED

Anderson, S. 1969. *Macrotus waterhousii*. American Society of Mammalogists. Mammalian Species 1:1–4.

Arizona Game and Fish Department. 2012. Arizona's State Wildlife Action Plan: 2012–2022. Arizona Game and Fish Department, Phoenix, Arizona. May 16, 2012. https://www.azgfd.com/PortalImages/files/wildlife/2012-2022_Arizona_State_Wildlife_Action_Plan.pdf

____. 2014. *Macrotus californicus*. Unpublished abstract compiled and edited by the Heritage Data Management System, Arizona Game and Fish Department, Phoenix, Arizona. 7 p.

Bell, G.P., G.A. Bartholomew and K.A. Nagy. 1986. The roles of energetics, water economy, foraging behavior, and geothermal refugia in the distribution of the bat, *Macrotus californicus*. Journal of Comparative Physiology 156:441–450.

Berry, R.D. and P.E. Brown. 1995. Natural history and reproductive behavior of the California leaf-nosed bat (*Macrotus californicus*). Bat Research News 36:49–50.

Bradley, R.D. and R.J. Baker. 2001. A test of the genetic species concept: cytochrome-b sequences and mammals. Journal of Mammalogy 82:960–973.

Bradshaw, G. 1961. Natural history study of the California leaf-nosed bats (*Macrotus californicus*). PhD dissertation submitted to the University of Arizona. 89 p.

_____. 1962. Reproductive Cycle of the California Leaf-Nosed Bat, *Macrotus californicus*. Science 136:645–646.

Brown, P.E. 2010. Roost Surveys and Monitoring for Lower Colorado River Bat Species. Submitted to the Lower Colorado River Multi-Species Conservation Program, Bureau of Reclamation, Boulder City, Nevada.

_____. 2011. Brown-Berry Biological Consulting, Blythe, California, personal communication.

Bureau of Land Management. 2014. Special Status Animals by Field Office. https://www.blm.gov/sites/blm.gov/files/documents/files/Programs_FishandWildlife_BLMCA%20Special%20Status%20Species.pdf

_____. 2017a. Threatened and Endangered Species Nevada. https://www.blm.gov/download/file/fid/23564

_____. 2017b. Updated Bureau of Land Management (BLM) Sensitive Species List for Arizona. https://www.blm.gov/download/file/fid/11852

Burland, T.M. and J. Worthington Wilmer. 2001. Seeing in the dark: molecular approaches to the study of bat populations. Biological Reviews 76:389–409.

California Department of Fish and Wildlife. 2016. Special Animals List. November 2018. https://nrm.dfg.ca.gov/FileHandler.ashx?DocumentID=109406&inline=1

Calvert, A. 2015. Post-Development Bat Monitoring of Habitat Creation Areas Along the Lower Colorado River – 2013–2014 Capture Surveys. Lower Colorado River Multi-Species Conservation Program, Bureau of Reclamation, Boulder City, Nevada.

Clutton-Brock, T.H. and D. Lukas. 2011. The evolution of social philopatry and dispersal in female mammals. Molecular Ecology 21(3):472–492.

Davis, B.L. and R.J. Baker. 1974. Morphometrics, evolution, and cytotaxonomy of mainland bats of the genus *Macrotus* (Chiroptera: Phyllostomatidae) (Abstract). Systematic Biology 23(1):26–39.

Earl, D.A. and B.M. von Holdt. 2012. STRUCTURE HARVESTER: a website and program for visualizing STRUCTURE output and implementing the Evanno method. Conservation Genetics Resources 4(2):359–361.

Ekblom, R. and J. Galindo. 2011. Applications of next generation sequencing in molecular ecology of non-model organisms. Heredity 107:1–15.

Environmental Conservation Online System. 2016. Listed Vertebrate Animals. http://ecos.fws.gov/ecp0/reports/ad-hoc-species-report?kingdom=V&status=E&status=T&status=EmE&status=EmT&status=SAE&status=SAT&mapstatus=1&fleadreg=on&fstatus=on&finvpop=on&header=Listed+Vertebrate+Animals

Environmental Systems Research Institute. 2011. ArcGIS Desktop: Release 10. Redlands, California.

Excoffier, L., P.E. Smouse, and J.M. Quattro. 1992. Analysis of molecular variance inferred from metric distances among DNA haplotypes: application to human mitochondrial DNA restriction data. Genetics 131(2):479–491.

Excoffier, L., G. Laval, and S. Schneider. 2005. Arlequin version 3.0: an integrated software package for population genetics data analysis. Evolutionary Bioinformatics Online 1:47–50.

Garner, T.W., S. Angelone, and P.B. Pearman. 2003. Genetic depletion in Swiss populations of *Rana latastei*: conservation implications. Biological Conservation 114(3):371–376.

Grant, W.S. 2015. Problems and cautions with sequence mismatch analysis and Bayesian skylane platos to infer historical demography. Heredity 2015:333–346.

Harpending, H. 1994. Signature of ancient population growth in a low-resolution mitochondrial DNA mismatch distribution. Human Biology 66(4):591–600.

Hoffman, F.G. and R.J. Baker. 2001. Systematics of bats of the genus *Glossophaga* (Chiroptera: Phyllostomidae) and phylogeography in *G. soricina* based on the cytochrome-*b* Gene. Journal of Mammalogy 82(4):1092–1101.

Hoffmeister, D.F. 1986. Mammals of Arizona. The University of Arizona Press, Tucson, Arizona. pp. 59–62.

Hoshino, A.A., J.P. Bravo, P.M. Nobile, and K.A. Morelli. 2012. Microsatellites as Tools for Genetic Diversity Analysis, Genetic Diversity in Microorganisms, Prof. Mahmut Caliskan (Ed.), InTech.

Hutchinson, D.W. 2003. Testing the central/peripheral model: analyses of microsatellite variability in the eastern collared lizard (*Crotaphytus collaris collaris*). The American Midland Naturalist 149(1):148–162.

International Union for the Conservation of Nature (IUCN). 2016. The IUCN Red List of Threatened Species. Version 2016-1. http://www.iucnredlist.org

IUCN (see International Union for the Conservation of Nature).

Jezkova, T., J.R. Jaeger, Z.L. Marshall, and B.R. Riddle. 2009. Pleistocene impacts on the phylogeography of the desert pocket mouse (*Chaetodipus penicillatus*). Journal of Mammalogy 90(2):306–320.

Jombart, T. and C. Collins. 2017. A tutorial for Discriminant Analysis of Principal Components (DAPC) using *adegenet* 2.1.0. https://github.com/thibautjombart/adegenet/blob/master/tutorials/tutorial-dapc.pdf

Jombart T., S. Devillard, and F. Balloux. 2010. Discriminant analysis of principal components: a new method for the analysis of genetically structured populations. BMC Genetics 11:1.

Kalinowski, S.T. 2011. The computer program STRUCTURE does not reliably identify the main genetic clusters within species: simulations and implications for human population structure. Heredity 106:625–632.

Lande, R. and J.F. Barrowclough. 1987. Effective population size, genetic variation, and their use in population management. Pages 87–123 *in* M.E. Soule (editor). Viable Populations for Conservation. Cambridge University Press, Cambridge, Massachusetts.

Leigh, J.W. and D. Bryant 2015. PopART: full-feature software for haplotype network construction. Methods in Ecology and Evolution 6(9):1110–1116.

Malausa, T., E. Gilles, E. Meglecz, S.D. Blanquart, C. Costedoat, V. Dubut, N. Pech, P. Castagnone-Sereno, C. Delye, N. Feau, P. Frey, B. Lung-Escarmant, P.G. Male, S. Ferreira and J. Martin. 2011. High-throughput microsatellite isolation through 454 GS-FLX titanium pyrosequencing of enriched DNA libraries. Molecular Ecology Resources 11(4):638–644.

Meglecz, E., F. Petenian, E. Danchin, A.C D'Acier, J.Y. Rasplus, and E. Faure. 2004. High similarity between flanking regions of different microsatellites detected within each of two species of Lepidoptera: *Parnassius apollo* and *Euphydryas aurinia*. Molecular Ecology 13:1693–1700.

Murray, K.L., and T.H. Fleming. 2008. Social structure and mating system of the buffy flower bat, *Erophylla sezekorni* (Chiroptera, Phyllostomidae). Journal of Mammology, 89(6):1391–1400.

Nei, M. 1972. Genetic distance between populations. The American Naturalist 106(949):283–292.

Paetkau, W., I. Calvert, I. Stirling and C. Strobeck. 1995. Microsatellite analysis of population structure in Canadian polar bears. Molecular Ecology 4:347–354.

Peakall, R. and P.E. Smouse. 2012. GenAlEx 6.5: genetic analysis in Excel. Population genetic software for teaching and research – an update. Bioinformatics 28:2537–2539.

Pierson, E.D. and W.E. Rainey. 1998. California leaf-nosed bat, *Macrotus californicus*. Pages 27-30 *in* B.C. Bolster (editor). Terrestrial Mammal Species of Special Concern in California, Draft Final Report. Prepared by P.V. Brylski, P.W. Collins, E.D. Pierson, W.E. Rainey, and T. E. Kucera. https://nrm.dfg.ca.gov/FileHandler.ashx?DocumentID=84523

Pritchard J.K., M. Stephens, and P. Donnelly. 2000. Inference of population structure using multilocus genotype data. Genetics 155:945–959.

Pritchard, J.K., X. Wen, and D. Falush. 2010. Documentation for structure software: version 2.3. http://www.ccg.unam.mx/~vinuesa/tlem09/docs/structure_doc.pdf

Rehn, J.A. 1904. A revision of the mammalian genus *Macrotus*. Proceedings of the Academy of Natural Sciences of Philadelphia 56(2):427–446.

Riddle, B.R., D.J. Hafner, L.F. Alexander, and J.R. Jaeger. 2000. Cryptic vicariance in the historical assembly of a Baja California Peninsular Desert biota. Procedures of the National Academy of Sciences 97:14438–14443. USA.

Rozas, J., A. Ferrer-Mata, J.C. Sánchez-DelBarrio, S. Guirao-Rico, P. Librado, S.E. Ramos-Onsins and A. Sánchez-Gracia. 2017. DnaSP 6: DNA sequence polymorphism analysis of large datasets. Molecular Biology and Evolution 34:3299–3302

Schwartz, M.K., L.S. Mills, Y. Ortega, L.F. Ruggiero, and F.W. Allendorf. 2003. Landscape location affects genetic variation of Canada lynx (*Lynx Canadensis*). Molecular Biology 12(7):1807–1816.

Selkoe, K.A. and R.J. Toonen. 2006. Microsatellites for ecologists: a practical guide to using and evaluating microsatellite markers. Ecology Letters 9:615–629.

Simmons, N.B. 2005. Order Chiroptera. Pages 312–529 *in* D.E. Wilson and D.M. Reeder (editors). Mammal Species of the World. The Johns Hopkins University Press, Baltimore, Maryland, USA.

Slatkin, M. and R.R. Hudson. 1991. Pairwise comparison of mitochondrial DNA sequences in stable and exponentially growing populations. Genetics 129(2):555–562.

Solari, S. 2018. *Macrotus californicus*. The IUCN Red List of Threatened Species 2018. e.T12652A22031754. http://dx.doi.org/10.2305/IUCN.UK.2018-2.RLTS.T12652A22031754.en

Tajima, F. 1989. Statistical method for testing the neutral mutation hypothesis by DNA polymorphism. Genetics 123(3):585–595.

Tamura, K., J. Dudley, M. Nei, and S. Kumar. 2007. MEGA4: molecular evolutionary genetics analysis (MEGA) software version 4.0. Molecular Biology and Evolution 24:1596–1599.

Thompson, R.S. and K.H. Anderson. 2000. Biomes of western North America at 18,000, 6,000 and 0 14C yr BP reconstructed from pollen and packrat midden data. Journal of Biogeography 27:555–584.

Van Oosterhout, C., W.F.D. Hutchinson, D. Wills, and P. Shipley. 2004. MICRO-CHECKER: Software for identifying and correcting genotyping errors in microsatellite data. Molecular Ecology Notes 4(3):535–538.

Waits, L.P. and S. Paetkau. 2005. Noninvasive genetic sampling tools for wildlife biologists: a review of applications and recommendations for accurate data collection. Journal of Wildlife Management 69(4):1419–1433.

Wright, S. 1965. The interpretation of population structure by F-statistics with special regard to systems of mating. Evolution 19(3):395–420.

Zane, L., L. Bargelloni, and T. Patarnello. 2002. Strategies for microsatellite isolation: a review. Molecular Ecology 11:1–16.

ATTACHMENT 1

Supplemental Tables

Table 1-1.—List of samples and localities

Locality	I.D.	Latitude	Longitude	Population #	Number of samples	Collected or museum
Warm Springs Natural Area	AWC-157 LVT4992	36.7113	-114.7124	1	2	Collected
Homestake Mine	MACA1 MACA2	35.2022	-114.5964	2	1	Collected
Hassayampa Preserve	JRH001 JRH002	34.9335	-112.6971	3	2	Collected
Bill Williams National Wildlife Refuge	JRH008 JRH011	34.273915	-114.051467	4	2	Collected
Californian Mine	MACA3 MACA4 MACA5 MACA6 MACA7 MACA8 MACA10 MACA11 MACA12 MACA13 MACA14 MACA15 MACA16 MACA17 MACA18	34.2676	-114.1558	5	15	Collected
Bumblebee	LVT10052 LVT10053 LVT10055	34.2283	-112.2283	6	2	Collected
‘Ahakhav Tribal Preserve	JRH004 JRH005	34.12901	-114.33348	7	2	Collected
Stonehouse Mine	MACA19 MACA20 MACA21 MACA22 MACA23 MACA24 MACA25 MACA26 MACA27 MACA28 MACA29 MACA30 MACA31 MACA33 MACA34 MACA35	33.5116	-114.7958	8	16	Collected

Table 1-1.—List of samples and localities

Locality	I.D.	Latitude	Longitude	Population #	Number of samples	Collected or museum
Cibola Valley Conservation Area	MACA38 MACA39 MACA40 MACA41	33.4095	-114.6591	9	4	Collected
Imperial National Wildlife Refuge	JRH006 JRH007 JRH009 JRH010	33.149357	-114.679377	10	4	Collected
3C Mine	MACA42 MACA43 MACA44 MACA45 MACA46 MACA47 MACA48 MACA49 MACA50 MACA51 MACA52 MACA53 MACA54 MACA55 MACA56	32.859	-114.5149	11	15	Collected
San Diego	SDMNH23963 SDMNH24830	32.773	-116.666	12	2	Museum
Picacho Peak	JRH012 JRH013 JRH014 JRH015 LVT10056 LVT 10057	32.632426	-111.3955264	13	6	Collected
Sawtooth Mountains	JRH016 JRH017 JRH018 JRH019 JRH020 JRH021 JRH022 JRH023 JRH024	32.584721	-111.7487523	14	9	Collected
Isla Tiburon Cave	NK42845 NK42858 NK42875 NK42877 NK42850	28.9954	-112.386	15	5	Museum

Table 1-1.—List of samples and localities

Locality	I.D.	Latitude	Longitude	Population #	Number of samples	Collected or museum
North of San Carlos	NK6643 NK17599 NK11131 NK80553 NK11124 NK11120	28	-111.1	16	6	Museum
Rio Cuchujaqui	NK5619	26.9451	-108.8843	17	1	Museum
Santa Marta	B02 B04 B06 B07 B08 B09 B11	25.4717	-111.0343	18	7	Museum
South of San Evaristo	MACA001 MACA002 MACA003 MACA513 MACA515 MACA802 MACA805	24.9082	-110.7198	19	7	Museum
Isla Espiritu Santo	LVT2433	24.4688	-110.3478	20	1	Museum
Base Camp	NK80553	28.009	-111.097	21	1	Museum

Table 1-2.—Median joining network node membership

Node label	Matching Sequences	Sample locality
NK11124	NK11124	San Carlos
	NK11131	San Carlos
	NK80553	San Carlos
	NK17599	San Carlos
LVT10053	LVT10053	Bumblebee
	6643	San Carlos
	NK42845	Isla Tiburon
NK42877	NK42877	Isla Tiburon
	NK42858	Isla Tiburon
MACA515	MACA515	South of San Evaristo
	MACA805	South of San Evaristo
B02	B02	Santa Marta
	B06	Santa Marta
	B11	Santa Marta
	B09	Santa Marta
	B04	Santa Marta
	B08	Santa Marta
	MACA003	South of San Evaristo
AWC157	AWC157	Warm Springs
	JRH001	Hassayampa Preserve
	JRH002	Hassayampa Preserve
	JRH008	Bill Williams National Wildlife Refuge
	JRH009	Imperial National Wildlife Refuge
	JRH010	Imperial National Wildlife Refuge
	JRH012	Picacho Peak
	JRH013	Picacho Peak
	JRH015	Picacho Peak
	JRH017	Sawtooth Mountains
	JRH018	Sawtooth Mountains
	JRH020	Sawtooth Mountains
	JRH022	Sawtooth Mountains
	LVT10055	Bumblebee
	LVT10056	Picacho Peak
	NK4992	Warm Springs Natural Area

Table 1-2.—Median joining network node membership

Node label	Matching Sequences	Sample locality
AWC157 (cont.)	MACA1	Homestake Mine
	MACA2	Homestake Mine
	MACA3	Californian Mine
	MACA4	Californian Mine
	MACA5	Californian Mine
	MACA6	Californian Mine
	MACA8	Californian Mine
	MACA12	Californian Mine
	MACA13	Californian Mine
	MACA15	Californian Mine
	MACA16	Californian Mine
	MACA19	Stonehouse Mine
	MACA21	Stonehouse Mine
	MACA23	Stonehouse Mine
	MACA25	Stonehouse Mine
	MACA26	Stonehouse Mine
	MACA27	Stonehouse Mine
	MACA28	Stonehouse Mine
	MACA30	Stonehouse Mine
	MACA31	Stonehouse Mine
	MACA34	Stonehouse Mine
	MACA39	Cibola Valley Conservation Area
	MACA40	Cibola Valley Conservation Area
	MACA41	Cibola Valley Conservation Area
	MACA44	3C Mine
	MACA46	3C Mine
	MACA47	3C Mine
	MACA48	3C Mine
	MACA49	3C Mine
	MACA50	3C Mine
	MACA51	3C Mine
	MACA52	3C Mine

Table 1-2.—Median joining network node membership

Node label	Matching Sequences	Sample locality
AWC157 (cont.)	MACA53	3C Mine
	MACA54	3C Mine
JRH006	JRH006	Imperial National Wildlife Refuge
	MACA7	Californian Mine
	MACA10	Californian Mine
	MACA11	Californian Mine
	MACA14	Californian Mine
	MACA17	Californian Mine
	MACA22	Stonehouse Mine
	MACA24	Stonehouse Mine
	MACA29	Stonehouse Mine
	MACA33	Stonehouse Mine
	MACA35	Stonehouse Mine
	MACA43	3C Mine
	MACA45	3C Mine
	MACA56	3C Mine
MACA001_11	MACA001_11	South of San Evaristo
	MACA002_11	South of San Evaristo
JRH014	JRH014	Picacho Peak
	JRH019	Sawtooth Mountains
	JRH021	Sawtooth Mountains
	JRH024	Sawtooth Mountains
JRH007	JRH007	Imperial National Wildlife Refuge
	JRH016	Sawtooth Mountains
MACA20	MACA20	Stonehouse Mine
	MACA38	Cibola Valley Conservation Area
	MACA42	3C Mine
	MACA55	3C Mine
JRH023	JRH023	Sawtooth Mountains
	LVT10057	Picacho Peak

Table 1-3.—Summary statistics for microsatellites
N = sample size, Na = number of alleles, Ho = observed heterozygosity, He = expected heterozygosity, d.f. = degrees of freedom, and ChiSq = chi-squared value

Population	Locus	N	Na	Ho	He	d.f.	ChiSq	P-value
Alamo	Locus1	1	1.000	0.000	0.000	Monomorphic		
	Locus2	1	2.000	1.000	0.500	1	1.000	0.317
	Locus3	1	2.000	1.000	0.500	1	1.000	0.317
	Locus4	1	2.000	1.000	0.500	1	1.000	0.317
	Locus5	1	1.000	0.000	0.000	Monomorphic		
Homestake Mine	Locus1	1	1.000	0.000	0.000	Monomorphic		
	Locus2	1	2.000	1.000	0.500	1	1.000	0.317
	Locus3	1	2.000	1.000	0.500	1	1.000	0.317
	Locus4	1	2.000	1.000	0.500	1	1.000	0.317
	Locus5	1	2.000	1.000	0.500	1	1.000	0.317
Hassayampa Preserve	Locus1	2	2.000	0.500	0.375	1	0.222	0.637
	Locus2	2	3.000	0.500	0.625	3	4.000	0.261
	Locus3	2	1.000	0.000	0.000	Monomorphic		
	Locus4	2	1.000	0.000	0.000	Monomorphic		
	Locus5	2	3.000	0.500	0.625	3	4.000	0.261
Bill Williams National Wildlife Refuge	Locus1	2	2.000	1.000	0.500	1	2.000	0.157
	Locus2	2	2.000	0.500	0.375	1	0.222	0.637
	Locus3	2	2.000	0.500	0.375	1	0.222	0.637
	Locus4	2	2.000	0.500	0.375	1	0.222	0.637
	Locus5	2	2.000	1.000	0.500	1	2.000	0.157
Californian Mine	Locus1	7	3.000	0.286	0.255	3	0.194	0.978
	Locus2	7	7.000	0.714	0.816	21	20.028	0.520
	Locus3	7	2.000	0.714	0.459	1	2.160	0.142
	Locus4	7	2.000	0.143	0.133	1	0.041	0.839
	Locus5	7	3.000	0.571	0.653	3	1.944	0.584
Bumblebee, Arizona	Locus1	2	1.000	0.000	0.000	Monomorphic		
	Locus2	2	3.000	0.500	0.625	3	4.000	0.261
	Locus3	2	1.000	0.000	0.000	Monomorphic		
	Locus4	2	2.000	1.000	0.500	1	2.000	0.157
	Locus5	2	2.000	1.000	0.500	1	2.000	0.157
‘Ahakhav Tribal Preserve	Locus1	2	1.000	0.000	0.000	Monomorphic		
	Locus2	2	4.000	1.000	0.750	6	6.000	0.423
	Locus3	2	2.000	1.000	0.500	1	2.000	0.157
	Locus4	2	1.000	0.000	0.000	Monomorphic		
	Locus5	2	3.000	0.500	0.625	3	4.000	0.261

Table 1-3.—Summary statistics for microsatellites
N = sample size, Na = number of alleles, Ho = observed heterozygosity, He = expected heterozygosity, d.f. = degrees of freedom, and ChiSq = chi-squared value

Population	Locus	N	Na	Ho	He	d.f.	ChiSq	P-value
Stonehouse Mine	Locus1	16	4.000	0.375	0.363	6	6.016	0.421
	Locus2	16	6.000	0.688	0.742	15	9.158	0.869
	Locus3	16	3.000	0.750	0.518	3	4.481	0.214
	Locus4	16	4.000	0.688	0.520	6	4.390	0.624
	Locus5	16	6.000	0.813	0.764	15	33.535	0.004
Cibola Valley Conservation Area	Locus1	4	3.000	0.750	0.531	3	1.440	0.696
	Locus2	4	5.000	0.750	0.750	10	11.111	0.349
	Locus3	4	3.000	1.000	0.594	3	4.000	0.261
	Locus4	4	4.000	1.000	0.656	6	4.000	0.677
	Locus5	4	3.000	1.000	0.625	3	4.000	0.261
Imperial National Wildlife Refuge	Locus1	4	2.000	0.500	0.375	1	0.444	0.505
	Locus2	4	3.000	0.750	0.625	3	1.000	0.801
	Locus3	4	2.000	0.750	0.469	1	1.440	0.230
	Locus4	4	2.000	0.250	0.219	1	0.082	0.775
	Locus5	4	3.000	0.750	0.625	3	1.000	0.801
3C Mine	Locus1	15	3.000	0.467	0.407	3	4.233	0.237
	Locus2	15	7.000	0.867	0.816	21	14.724	0.837
	Locus3	15	2.000	0.467	0.358	1	1.389	0.239
	Locus4	15	3.000	0.933	0.571	3	11.484	0.009
	Locus5	15	7.000	0.800	0.740	21	44.171	0.002
San Diego	Locus1	2	2.000	0.500	0.375	1	0.222	0.637
	Locus2	2	2.000	0.500	0.375	1	0.222	0.637
	Locus3	2	2.000	0.500	0.375	1	0.222	0.637
	Locus4	2	2.000	1.000	0.500	1	2.000	0.157
	Locus5	2	4.000	1.000	0.750	6	6.000	0.423
Picacho Peak	Locus1	2	2.000	0.500	0.375	1	0.222	0.637
	Locus2	2	2.000	1.000	0.500	1	2.000	0.157
	Locus3	2	2.000	0.500	0.375	1	0.222	0.637
	Locus4	2	2.000	0.500	0.375	1	0.222	0.637
	Locus5	2	2.000	0.500	0.375	1	0.222	0.637
Sawtooth Mountains	Locus1	4	2.000	0.500	0.500	1	0.000	1.000
	Locus2	4	3.000	0.750	0.594	3	2.333	0.506
	Locus3	4	2.000	0.750	0.469	1	1.440	0.230
	Locus4	4	2.000	1.000	0.500	1	4.000	0.046
	Locus5	4	5.000	0.500	0.750	10	12.444	0.256

Table 1-3.—Summary statistics for microsatellites
N = sample size, Na = number of alleles, Ho = observed heterozygosity, He = expected heterozygosity, d.f. = degrees of freedom, and ChiSq = chi-squared value

Population	Locus	N	Na	Ho	He	d.f.	ChiSq	P-value
Isla Tiburon Cave	Locus1	5	3.000	0.200	0.340	3	10.000	0.019
	Locus2	5	7.000	1.000	0.820	21	25.000	0.247
	Locus3	5	3.000	0.800	0.580	3	2.800	0.423
	Locus4	5	2.000	1.000	0.500	1	5.000	0.025
	Locus5	5	4.000	0.800	0.640	6	3.800	0.704
North of San Carlos	Locus1	3	2.000	0.333	0.278	1	0.120	0.729
	Locus2	3	5.000	0.667	0.778	10	12.000	0.285
	Locus3	3	3.000	1.000	0.611	3	3.000	0.392
	Locus4	3	2.000	0.333	0.278	1	0.120	0.729
	Locus5	3	5.000	0.667	0.778	10	12.000	0.285
Rio Cuchujaqui	Locus1	1	2.000	1.000	0.500	1	1.000	0.317
	Locus2	1	1.000	0.000	0.000	Monomorphic		
	Locus3	1	1.000	0.000	0.000	Monomorphic		
	Locus4	1	2.000	1.000	0.500	1	1.000	0.317
	Locus5	1	1.000	0.000	0.000	Monomorphic		
South of San Evaristo	Locus1	7	2.000	0.429	0.337	1	0.521	0.471
	Locus2	7	6.000	0.857	0.776	15	18.958	0.216
	Locus3	7	3.000	0.857	0.561	3	4.238	0.237
	Locus4	7	3.000	0.714	0.500	3	2.160	0.540
	Locus5	7	4.000	0.000	0.694	6	21.000	0.002
Isla Santo Espiritu	Locus1	7	2.000	0.143	0.337	1	2.320	0.128
	Locus2	7	5.000	0.857	0.622	10	3.938	0.950
	Locus3	7	2.000	0.571	0.408	1	1.120	0.290
	Locus4	7	3.000	0.857	0.571	3	3.938	0.268
	Locus5	7	4.000	1.000	0.643	6	7.000	0.321
Base Camp	Locus1	1	1.000	1.000	0.000	1	1.000	0.317
	Locus2	1	2.000	2.000	0.693	1	1.000	0.317
	Locus3	1	2.000	2.000	0.693	1	1.000	0.317
	Locus4	1	2.000	2.000	0.693	1	1.000	0.317
	Locus5	1	2.000	2.000	0.693	1	1.000	0.317